
Why Does Reasoning Length Converge?

Unveiling the Underfitting-Overfitting Trade-off in Chain-of-Thought

Zeyu Gan¹ Yi Hao¹ Yong Liu¹

Abstract

Test-time scaling, primarily manifested through multi-step Chain-of-Thought (CoT) reasoning via Reinforcement Learning (RL), has emerged as a pivotal paradigm for enhancing the reasoning capabilities of Large Language Models (LLMs). However, a significant theoretical gap persists: traditional token-level analysis fails to capture the macroscopic dynamics of reasoning-level scaling. To address this, we introduce CoT-Space, a novel theoretical framework that recasts the reasoning process from a discrete token-prediction task to an optimization process within a continuous, reasoning-level semantic space. By modeling the reasoning trajectory from both noise and risk perspectives and revitalizing foundational principles from classical learning theory, we demonstrate that the observed convergence to an optimal CoT length is a natural consequence of the fundamental trade-off between underfitting and overfitting. We further utilize RL as a tool to elicit and verify these results in our experiments. Our findings provide a mechanistic explanation for the internal test-time scaling via RL, offering a principled theoretical foundation to optimize reasoning trajectories in modern LLMs. We open-source our code at <https://github.com/ZyGan1999/CoT-Space>.

1. Introduction

Improving the reasoning capabilities of Large Language Models (LLMs) is pivotal in modern AI research. The most well-known framework for this is Chain-of-Thought (CoT) (Wei et al., 2022b), which elicits multi-step reasoning. A promising strategy to enhance CoT is “test-time scaling” (Chen et al., 2025b; Jiang et al., 2024), which can be broadly categorized into external and internal meth-

ods. External methods, such as tree-based strategies (Yao et al., 2023; Zhang et al., 2024; Wan et al., 2024) and self-consistency (Wang et al., 2022), augment the model’s inference-time output via searching (Gan et al., 2025). While internal test-time scaling methods embed the reasoning capability directly into the model’s inference process via post-training, typically utilizing Reinforcement Learning (RL) with a high-level outcome reward.

Recent breakthroughs from models like DeepSeek’s R1 (DeepSeek-AI, 2025), OpenAI’s o1 and o3 (OpenAI, 2024; 2025), and Qwen’s QwQ (Qwen, 2024) have spotlighted the power of internal test-time scaling. This paradigm, also known as *zero*-like training, involves applying RL directly to a pre-trained model, bypassing supervised tuning. The empirical results are compelling, showing that a high-level objective can guide a policy to discover an optimal strategy on its own. This reveals an interesting insight: the *zero*-like training process is actually guiding the model to find an optimal inference policy.

As illustrated in Figure 1, *zero*-like training for LLM reasoning is analogous to the classical strategy optimization process. In a classic RL task like Bricks Breaker¹ shown in subgraph (a), the agent’s goal is to break more bricks. Without explicit instructions on specific strategies, the agent may discover a highly effective method, such as hitting the ball behind the top row of bricks to achieve a higher score. Similarly, in the context of LLM reasoning, as shown in subgraph (b), the policy model is given the broad goal of providing a correct answer. As RL training progresses, the model converges on an optimal CoT length, demonstrating its ability to optimize via a simple, high-level reward signal.

A variety of RL-based methods have been developed to improve *zero*-like post-training, including GRPO (Shao et al., 2024), VC-PPO (Yuan et al., 2025), DAPO (Yu et al., 2025), and VAPO (Yue et al., 2025b). However, despite these empirical successes, our theoretical understanding of internal test-time scaling remains shallow (Gan et al., 2026). For instance, the convergence on an optimal CoT length during training, also known as the “overthinking” phenomenon (Sui

¹Gaoling School of Artificial Intelligence, Renmin University of China, Beijing, China. Correspondence to: Yong Liu <liyonggsai@ruc.edu.cn>.

¹Bricks Breaker is a video game, the goal is to destroy the bricks by shooting a ball at them.



Figure 1. Analogy between strategy discovery in classical RL and LLM reasoning. (a) In classical RL, an agent with a high-level goal (e.g., break more bricks) discovers an effective strategy through exploration to maximize its reward. (b) Similarly, an LLM policy with the goal of providing correct answers autonomously learns that generating a suitable CoT is an effective strategy.

et al., 2025), lacks a clear mechanistic explanation.

This chasm between empirical success and theoretical understanding is alarming. It stands in stark contrast to old-school machine learning, where decades of research have forged a robust theoretical bedrock. Unfortunately, foundational principles appear to falter when applied to the complex, multi-step nature of LLM reasoning. This prompts the critical question that motivates our work: **Are these time-tested theories truly obsolete in this new era, or do we merely lack the conceptual framework to bridge them to the unique dynamics of LLM reasoning?** We argue for the latter, positing that by shifting our analytical perspective, we can revitalize these foundational theories and use them to build a principled understanding of LLM reasoning.

The central barrier to this goal is twofold. **First, a fundamental misalignment exists between token-level analytical frameworks and the reasoning-level nature of CoT**, where actions are complete thoughts rather than single tokens. **Second, a conceptual gap separates the discrete world of language from the continuous mathematics underpinning classic learning theory**, hindering the application of its powerful analytical tools. To resolve both challenges, we introduce **CoT-Space**, a novel reasoning-level theoretical framework for LLM reasoning via RL. Served as a conceptual framework, we aim to build a theoretical bridge that connects the empirical phenomena of LLM reasoning with foundational principles of classical machine learning. Our framework first defines a reasoning-level state space to

align the analytical framework with CoT’s structure. Subsequently, we prove this space converges to a continuous manifold, a key result that recasts reasoning as an optimization process. By leveraging this continuous perspective, we are then able to conduct analyses that explain the convergence of an optimal CoT length from both noise and risk perspectives. We reveal that this convergence is actually an underfitting-overfitting trade-off during CoT generations.

The remainder of this paper is structured as follows. In Section 2, we provide a systematic analysis of the misalignment between the current token-level inference formulation and the reasoning-level nature of CoT generations. Subsequently, we introduce our reasoning-level theoretical framework, CoT-Space. We then leverage this framework in Section 3 to analyze the convergence of CoT length in the reasoning process from the perspective of noise and risk, demonstrating its potential theoretical value. We perform empirical validation of our theoretical insights in Section 4. Following this, we briefly review related works in Section 5 and finally conclude the paper in Section 6.

2. CoT-Space: A Reasoning-Level Theoretical Framework

This section presents a systematic analysis of CoT reasoning. We first discuss existing misalignment (Subsection 2.1), then introduce our reasoning-level framework, CoT-Space (Subsection 2.2), and finally prove its continuum nature to establish the theoretical foundation (Subsection 2.3).

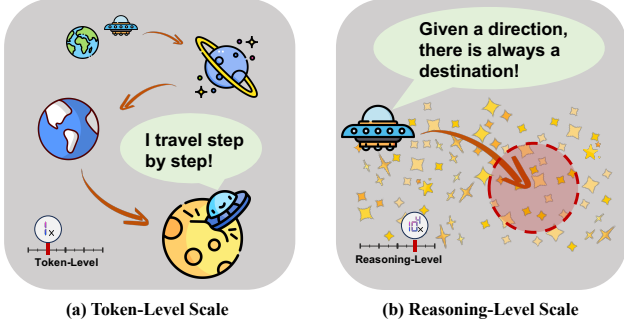


Figure 2. **Token-level vs. Reasoning-level perspectives.** (a) The token-level view treats the generation process as a path through discrete states. (b) The reasoning-level view zooms out, approximating the dense state space as continuous.

2.1. From Token-Level to Reasoning-Level Perspective

The conventional framework for LLM reasoning is fundamentally misaligned with the reasoning-level nature of CoT scenarios. This misalignment stems from modeling autoregressive language generation as a token-level Markov Decision Process (MDP) (Setlur et al., 2025): $\mathcal{M}(\mathcal{S}, \mathcal{A}, r, H)$, where \mathcal{S} is the state space of existing token sequences, \mathcal{A} is the action space representing the token dictionary, r is the reward function guiding generation, and H is the token budget. In this standard formulation, a policy $\pi : \mathcal{S} \rightarrow \mathcal{A}$ produces the next token $a = \pi(s)$ to extend the current sequence s . While inherited from classic RL tasks, this formulation presents a significant challenge regarding the token-level state space \mathcal{S} in natural language, as we assert next (details in Appendix A):

Assertion 2.1. The token-level state space \mathcal{S} of natural language exhibits **exponential growth** and **discrete topology**.

To address this, we propose shifting the analytical perspective from the microscopic token level to the macroscopic reasoning level. We posit that while the token-level state space is discrete and sparse, the reasoning-level state space, which is formed by abstract thoughts, can be approximated as a continuous manifold. This is analogous to interstellar travel: while individual stars (tokens) are discrete, the galaxy (semantic space) appears continuous from a distance. This “zoom-out” perspective allows us to apply continuous optimization tools to analyze the reasoning process, as discussed in Figure 2.

2.2. Formulation of CoT-Space

To formalize this conceptual “zoom out” framework, we define the following constructs. Note that these definitions rely on abstract semantic equivalence, serving as theoretical tools rather than computable functions.

Based on the CoT setting, where the output is generated step-by-step and consists of multiple intermediate thoughts,

a reasoning state is defined as follows.

Definition 2.2. (CoT reasoning state.) Given a query q and a set of intermediate abstract steps $\xi_o = [\xi_1, \xi_2, \dots, \xi_t]$, the current reasoning state is defined as $s_o = (q, \xi_o)$.

Definition 2.2 establishes the concept of reasoning-level state. We then introduce a special class of states that represent successful problem solutions, which we call *minimums*.

Definition 2.3. (Minimums in reasoning space.) Given a query q with a definite golden answer ϕ . Let Ξ_q be the set of all reasonable intermediate reasoning processes for query q . Then the minimums of the reasoning space are defined as $\mathcal{M}_q = \{(q, \xi, \phi) \mid \xi \in \Xi_q\}$.

By Definition 2.3, minimums are states where the query has been successfully solved. For any intermediate reasoning state, we can then define which minimums are reachable.

Definition 2.4. (Reachable minimums.) Given a query q with a definite golden answer ϕ , and an incomplete set of intermediate reasoning steps $\xi_o = [\xi_1, \xi_2, \dots, \xi_t]$. The reachable minimums are defined as $\mathcal{R}_q^o = \{(q, \xi, \phi) \mid \xi_o \sqsubseteq \xi \text{ and } \xi \in \Xi_q\}$, where $a \sqsubseteq b$ represents that a is prefix of b .

Definition 2.4 establishes the concept of reachable minimums. This concept represents the set of successful reasoning paths that can be completed from the current state. We then quantify the distance between a state and its reachable minimums and define the nearest minimum.

Definition 2.5. (Reachable distance and nearest reachable minimum.) Given a query q with a definite golden answer ϕ , and a reasoning state s_o on this query, the reachable distance between the s_o and a reachable minimum is defined as $\text{dist}(s_o, m) = |\xi| - |\xi_o|$, where $m \in \mathcal{R}_q^o$, ξ and ξ_o are intermediate steps of m and s_o respectively, $|\cdot|$ represents the length of a vector. The nearest minimum is defined as $m_o^* = \arg \min_{m \in \mathcal{R}_q^o} \text{dist}(s_o, m)$.

Definition 2.5 quantifies the number of reasoning steps required to reach the closest successful solution from a given state. Finally, we define a reasoning loss to characterize the gap between the current state and the optimal solution.

Definition 2.6. (Reasoning loss.) Given a query q with a definite golden answer ϕ , and a reasoning state s_o on this query, there exists a loss function C that quantifies the distance of s_o towards its nearest reachable minimum, which satisfies: for two different states s_i, s_j , $C(s_i, q) < C(s_j, q)$ if and only if $\text{dist}(s_i, m_i^*) < \text{dist}(s_j, m_j^*)$. Specially, $\forall m \in \mathcal{M}_q$, $C(m, q) = 0$.

Definition 2.6 conceptualizes the reasoning process as an optimization process. The function $C(\cdot, \cdot)$ acts as a proxy for the distance to a correct solution, where a lower loss

indicates a more advanced stage of reasoning. Taking Figure 3(a) as instance, in this transition, m_i, m_j and m_k are all reachable minimums for the current state s_0 . However, the possible next states of s_0 , which are denoted as s_i, s_j and s_k (Here we refer to the three realizations s_{i_1}, s_{i_2} and s_{i_3} all as s_i for simplicity). These intermediate states differ in their distance to its corresponding minimums ($\text{dist}(s_i, m_i) < \text{dist}(s_j, m_j) < \text{dist}(s_k, m_k)$). Given the same query q , the reasoning losses thus satisfy $C(s_i, q) < C(s_j, q) < C(s_k, q)$.

With this complete reasoning-level analytical framework established, we resolve the misalignment between token-level RL and the reasoning-level CoT paradigm. We now turn to prove the continuum nature of the reasoning-level state space, thus yielding the rationality of CoT-Space.

2.3. On the Continuum Nature of the Reasoning-Level State Space

The essence of reasoning lies in the semantic meaning of conceptual steps, not in the specific tokens used to express them. A single reasoning step, such as ‘‘calculating the total weekly pages’’ can be realized by a vast number of distinct token sequences ξ_{i_1}, ξ_{i_2} and ξ_{i_3} , as shown in Figure 3(a).

From token-level perspective, different token sequences correspond to distant, discrete states. However, in a higher-dimensional semantic space, they are nearly identical. The CoT-Space framework posits that as the reasoning length increases, the number of semantically meaningful states grows so rapidly that the space they inhabit can be treated as a continuous manifold. This density arises from the expressive redundancy of language: the number of valid token-level paths to achieve a reasoning goal grows exponentially with the available token budget.

To formalize this, we introduce the following definitions and a key assumption.

Definition 2.7. (Semantic equivalence set.) For an abstract reasoning step ξ_l , its semantic equivalence set $\mathcal{V}(\xi_l, k)$ is the collection of all token sequences $\tau \in \mathcal{A}^k$ with length k that are semantically equivalent to ξ_l , defined as: $\mathcal{V}(\xi_l, k) = \{\tau \in \mathcal{A}^k \mid \text{Decode}(\tau) \equiv \xi_l\}$, where \mathcal{A}^k is the space of all token sequences with length k , and $\text{Decode}(\cdot)$ is an abstract function mapping a token sequence to its semantic meaning.

Definition 2.8. (Reasoning state density.) Within a fixed semantic volume $\mathcal{V}_{\text{semantic}}$, the set of all valid, reachable reasoning states of reasoning token amount K is denoted by $\mathcal{S}_{\text{reasoning}}^{(K)}$. The state density $\rho(K)$ is defined as the number of states per unit of semantic volume: $\rho(K) = |\mathcal{S}_{\text{reasoning}}^{(K)}| / |\mathcal{V}_{\text{semantic}}|$.

To substantiate our claim that this density grows exponentially, we propose the following assumption.

Assumption 2.9. (Exponential expressive redundancy of language.) For any non-trivial reasoning step ξ_l , the size of its semantic equivalence set $|\mathcal{V}(\xi_l, k)|$, when realized by k tokens, grows exponentially with k . That is, there exists a constant $c > 1$ such that: $|\mathcal{V}(\xi_l, k)| \geq c^k$.

We provide a proof for this assumption via the Kolmogorov Complexity from both a construction perspective and an information-theoretic perspective in Appendix C.1. This assumption acts as a foundational theoretical posit for our framework, grounded in the combinatorial nature of language where adding tokens exponentially increases the space of semantically equivalent expressions.

Based on these foundations, we can now formally state the lemma that justifies the continuum approximation of the reasoning-level state space.

Lemma 2.10. (Continuum convergence of reasoning-level state space.) Under Assumption 2.9, in a D -dimensional semantic space, the reasoning-level state density, denoted as $\rho(K)$, increases exponentially with the reasoning token amount K , formally $\rho(K) = \Theta(c^K)$. Let $s_i \bowtie s_j$ denotes that s_i, s_j are nearest neighbor states of each other, the expected nearest neighbor distance of the semantic manifold is inversely related to the reasoning state density, formally $\mathbb{E}_{s_i \bowtie s_j}[\text{dist}(s_i, s_j)] \propto \rho(K)^{-1/D}$.

The proof is provided in Appendix C.2. In Lemma 2.10, we established that the reasoning-level state space converges to a continuous semantic manifold in a macroscopic limit. Here, we further quantify the total ‘‘gap’’ between an ideal continuous update and the best possible discrete step, demonstrating that this gap vanishes as the total reasoning token amount K increases.

A visualization for this analysis is presented in Figure 3(b). Consider the original discrete reasoning state space \mathcal{S} and its corresponding continuous manifold $\tilde{\mathcal{S}}$, where $\mathcal{S} \subset \tilde{\mathcal{S}}$. For a state transition starting from s , let \vec{v}_{ideal} be the ideal optimization vector with domain on $\tilde{\mathcal{S}}$, and let \vec{v}_{real} be the best achievable discrete optimization vector with domain on \mathcal{S} . Since \vec{v}_{real} serves as an approximation for \vec{v}_{ideal} , the total vector error is $\vec{\epsilon}_{\text{total}}(s) = \vec{v}_{\text{real}} - \vec{v}_{\text{ideal}}$. We can decompose the analysis of this error into two components: the error in direction (angle) and the error in size (magnitude).

Definition 2.11. (Continuum errors.) The total error for continuum approximation is characterized by two components: **(1) The angular error**, $\epsilon_A(s)$, defined as the angle between \vec{v}_{ideal} and \vec{v}_{real} . **(2) The magnitude error**, $\epsilon_M(s)$, defined as difference in norms: $\epsilon_M(s) = \|\vec{v}_{\text{real}}\| - \|\vec{v}_{\text{ideal}}\|$.

We will further show the convergence relationship between the continuum errors and the density, thereby revealing the rationality of the reasoning-level state space continuous approximation.

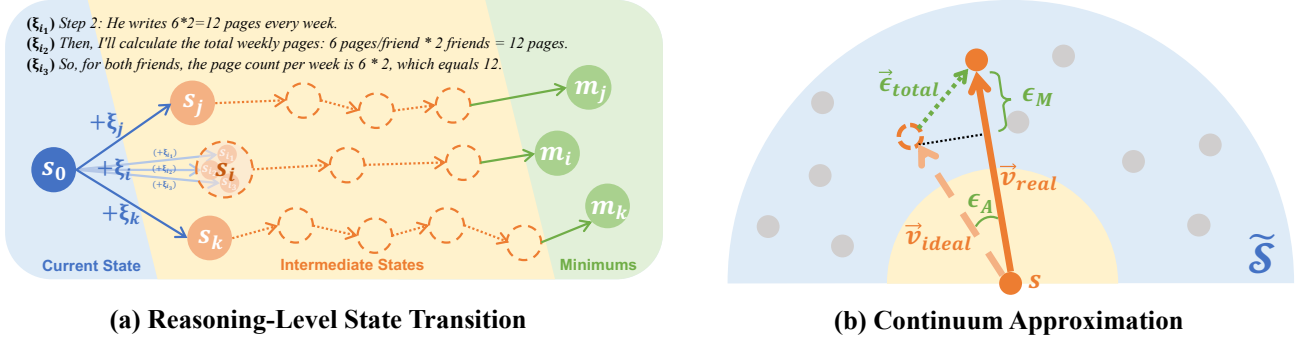


Figure 3. **Illustration of CoT-Space.** (a) Different reasoning steps (ξ_i, ξ_j, ξ_k) lead to different minimums (m_i, m_j, m_k), while one step can have multiple token-level realizations ($\xi_{i_1}, \xi_{i_2}, \xi_{i_3}$). (b) The discrete state space \mathcal{S} (dots) is approximated as a continuous manifold $\hat{\mathcal{S}}$ (blue area), where the real optimization vector (\vec{v}_{real}) approximates the ideal one (\vec{v}_{ideal}).

Theorem 2.12. (Convergence of the continuum error). The expected angular error $\mathbb{E}[\epsilon_A(s)]$ and expected magnitude error $\mathbb{E}[\epsilon_M(s)]$ are both upper-bounded by a function that is inversely related to the reasoning state density $\rho(K)$, formally $\mathbb{E}[\epsilon_A(s)] \leq \mathcal{O}(\rho(K)^{-\frac{1}{D}})$ and $\mathbb{E}[\epsilon_M(s)] \leq \mathcal{O}(\rho(K)^{-\frac{1}{D}})$.

The proof is provided in Appendix C.4. Theorem 2.12 demonstrates that the total error in approximating a true gradient vector with the best possible discrete step is bounded and converges to zero as the model’s expressive capacity (K) increases. By ensuring that for a sufficiently large K , a discrete step vector \vec{v}_{real} that is an arbitrarily accurate approximation of the ideal vector \vec{v}_{ideal} can always be found. With the continuum nature of the reasoning space established, we bridge the gap between discrete language generation and classical results. Specifically, it allows us to conceptualize a smooth reasoning loss landscape and thus define a corresponding gradient, enabling us to model the generation of a new reasoning step as a descent-like update.

Building upon this, we can frame the entire reasoning process as a trajectory in a continuous state space, and link many LLM phenomena, such as hallucination, prompt sensitivity, emergent abilities, and effectiveness of external slow-thinking strategies, with classical theoretical results. A brief discussion is provided in Appendix F. In the next section, we take the “overthinking” phenomenon as a detailed example to reveal the potential of CoT-Space for revitalizing the classical theoretical results.

3. Analytical Applications within CoT-Space

This section utilizes the CoT-Space framework and combines classic learning theories to analyze the “overthinking” phenomenon, thus yielding the potential of CoT-Space. We provide a theoretical foundation by examining the issue through two lenses: optimization noise (Subsection 3.1) and reasoning risk (Subsection 3.2), followed by a summary of

our theoretical insights (Subsection 3.3).

3.1. Reasoning as Optimization: A Perspective of Noise

Leveraging the continuous nature of CoT-Space, we frame LLM reasoning as an optimization process analogous to ML, as shown in Figure 4. In this analogy, an LLM policy iteratively refines its reasoning state towards a solution, much like an optimizer updates parameters. This perspective allows us to apply further analysis via noise.

To characterize the random exploration during inference time, we model the optimization of LLM reasoning as a noisy reasoning loss descent process. Specifically, we treat the step-by-step generation of a CoT with length L as a discretization of a continuous stochastic process. We formulate this mathematically as a Stochastic Differential Equation (SDE) on the continuous manifold (details in Appendix C.5), where σ represents the noise scale of the optimization trajectory. To theoretically derive the relationship between σ and L , we bridge the discrete and continuous perspectives by equating the noise variance of a single reasoning step, and give the following theorem as an intuitive result.

Theorem 3.1. (Relationship between noise scale and CoT length.) In a given optimization space, the noise scale σ is inversely proportional to the reasoning length L , i.e. $\sigma \propto \frac{1}{L}$.

The proof is provided in Appendix C.5. Theorem 3.1 clarifies the relationship between the noise σ and the CoT length L in the reasoning process. According to the sharpness-aware minimization principles (Keskar et al., 2016), given a reasoning task, there must exist an optimal noise scale σ_{opt} , which corresponds to an optimal CoT length $L_{\text{opt}} \propto \frac{1}{\sigma_{\text{opt}}}$. In essence, Theorem 3.1 provides a fundamental basis for why an optimal CoT length is crucial for effective reasoning, highlighting its role in introducing the right amount of noise to achieve a flat, high-quality, and generalizable solution.

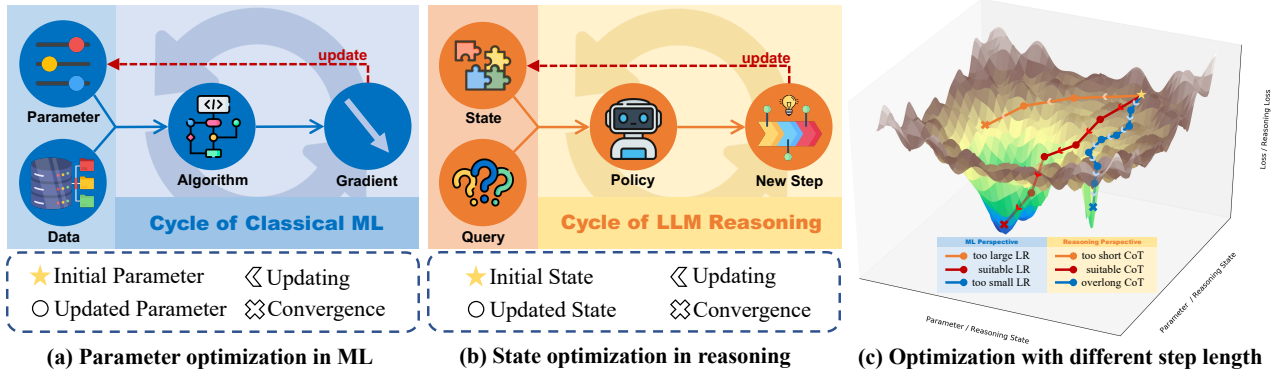


Figure 4. **Modeling LLM reasoning as an optimization process.** (a) Traditional ML performs parameter optimization by updating model weights. (b) Our framework models reasoning as state optimization, where new reasoning steps iteratively update the current state. (c) This panel visualizes this process on a reasoning loss landscape, where the CoT length is analogous to a learning rate; an optimal value is crucial for converging to a high-quality, generalizable solution.

3.2. Reasoning and Generalization: From Noise to Risk

The previous section fundamentally considered reasoning from the perspective of noise. We now provide a deeper analysis to link this noise perspective with the risk in CoT reasoning. By modeling the reasoning process as a stochastic dynamical system, we derive an information-theoretic generalization bound that explicitly characterizes the trade-off between optimization drift and information complexity.

3.2.1. STOCHASTIC DYNAMICS OF REASONING

We formalize the generation of a CoT sequence as a discrete-time approximation of a continuous stochastic process on a semantic manifold $\mathcal{M} \subseteq \mathbb{R}^d$. Let $s_t \in \mathbb{R}^d$ denote the reasoning state at step t , and $q \sim \mathcal{D}$ be the input query drawn from a data distribution \mathcal{D} . The Reasoning Loss $C(s, q) : \mathbb{R}^d \times \mathcal{Q} \rightarrow \mathbb{R}$ is the semantic distance between the current state s and the ground-truth solution for query q .

To visually illustrate our conclusions, we performed a more refined discretization model of SDE for equation (39) as follows. It’s worth noting that we can easily obtain similar conclusions under continuous settings.

$$s_t = s_{t-1} - \eta \nabla C(s_{t-1}, q) + \sigma \zeta_t, \quad \zeta_t \sim \mathcal{N}(0, I_d),$$

where $\eta > 0$ is the step size, and $\sigma \geq 0$ represents the Reasoning Noise Scale. The drift term $-\nabla C(s_{t-1}, q)$ drives the reasoning process towards semantic correctness, while the diffusion term $\sigma \zeta_t$ introduces necessary exploration.

To rigorously analyze the impact of reasoning noise, we first formally distinguish between the deterministic (greedy) reasoning trajectory and the stochastic (exploratory) reasoning trajectory derived from our SDE framework, following the settings of Wang & Mao (2022).

Definition 3.2. (Noise-free trajectory.) Let $\mathcal{T}^* =$

$\{s_0^*, s_1^*, \dots, s_T^*\}$ denote the deterministic reasoning trajectory generated when the noise scale is set to zero ($\sigma = 0$). This trajectory corresponds to a greedy decoding process or a standard gradient descent path in the semantic space, governed by the recurrence:

$$s_t^* = s_{t-1}^* - \eta \nabla C(s_{t-1}^*, q), \quad \text{with } s_0^* = s_{\text{initial}}.$$

We refer to s_T^* as the Deterministic Baseline Solution, which serves as the reference point for our stability analysis.

Definition 3.3. (Noisy trajectory.) Let $\mathcal{T} = \{s_0, s_1, \dots, s_T\}$ denote the stochastic reasoning trajectory generated under a non-zero noise scale $\sigma > 0$. This trajectory evolves according to the full SDE discretization:

$$s_t = s_{t-1} - \eta \nabla C(s_{t-1}, q) + \sigma \zeta_t, \quad \text{with } s_0 = s_{\text{initial}},$$

where $\zeta_t \sim \mathcal{N}(0, I_d)$ represents the independent Gaussian noise injected at each step.

Definitions 3.2 and 3.3 conceptualize the role of noise in the reasoning process. We subsequently analyze the reasoning risk in the following subsections.

3.2.2. REASONING RISK ANALYSIS VIA NOISE

A core challenge in reasoning is avoiding overfitting to the superficial patterns of a specific prompt (i.e., prompt sensitivity), which leads to poor generalization on unseen queries. To quantify this, we introduce the concept of Thought Dispersion, inspired by the gradient dispersion in SGD analysis.

Definition 3.4. (Thought dispersion.) The Thought Dispersion $\mathbb{V}_t(s)$ at state s quantifies the variance of the reasoning direction induced by different queries relative to the expected semantic drift:

$$\mathbb{V}_t(s) \triangleq \mathbb{E}_{q \sim \mathcal{D}} \left[\left\| \nabla C(s, q) - \mathbb{E}_{q' \sim \mathcal{D}} [\nabla C(s, q')] \right\|_2^2 \right].$$

Intuitively, a high $\mathbb{V}_t(s)$ indicates that the reasoning step is highly sensitive to the specific instance q , implying a higher risk of memorizing instance-specific shortcuts rather than learning robust reasoning patterns. We now state our main theorem, which bounds the expected population risk $R_{pop} \triangleq \mathbb{E}_{q,\zeta}[C(s_T, q)]$ in terms of the noise scale σ .

Theorem 3.5. (Noise-Generalization trade-off.) *Assume the reasoning loss function $C(\cdot, q)$ is Γ -subgaussian and β -smooth. For a reasoning process of length L , the expected population risk is upper-bounded by:*

$$\mathbb{E}(R_{pop}) \leq \underbrace{R_{emp}^* + \frac{\beta L \sigma^2 d}{2}}_{(I) \text{ Optimization Drift}} + \underbrace{\sqrt{\frac{2\Gamma^2}{n} \sum_{t=1}^L \frac{d}{2} \log \left(1 + \frac{\eta^2 \mathbb{E}[\mathbb{V}_t(s_{t-1})]}{d\sigma^2} \right)}}_{(II) \text{ Information Complexity}},$$

where n is the number of training examples, R_{emp}^* is the empirical risk of the deterministic (greedy) path, and the expectation in Term (II) is taken over the reasoning trajectory.

The proof is provided in Appendix C.6. Theorem 3.5 reveals that the expected population risk is governed by a fundamental trade-off between two competing components, which we formalize as (I) Optimization Drift and (II) Information Complexity. This trade-off is governed by the reasoning noise scale σ and the reasoning length L . Recall Theorem 3.1, we can roughly derive that the order of Term (I) is $\mathcal{O}(\sigma)$ or $\mathcal{O}(\frac{1}{L})$, and the order of Term (II) is $\mathcal{O}\left(\sqrt{\frac{1}{\sigma} \log \frac{1}{\sigma}}\right)$ or $\mathcal{O}(\sqrt{L \log L})$.

Term (I): Optimization Drift (Underfitting Regime). Analogous to Bias, this term quantifies the deviation from the optimal descent path. As $\sigma \rightarrow \infty$, this term dominates as excessive noise disrupts the effective semantic drift. The trajectory is forced to diverge from the correct solution, preventing convergence and resulting in high empirical risk.

Term (II): Information Complexity (Overfitting Regime). Analogous to Variance, this term bounds the mutual information between the reasoning path and the input. As $\sigma \rightarrow 0$ (approximating greedy decoding), this term diverges, meaning the policy encodes excessive instance-specific details. This leads to brittle reasoning chains that are highly sensitive to prompt perturbations, resulting in poor generalization.

Consequently, there exists a strictly positive optimal noise scale $\sigma^* > 0$ that minimizes the total bound. This provides a theoretical justification for the empirical success of sampling-based strategies (e.g., Self-Consistency) over greedy decoding, suggesting that controlled stochasticity is a prerequisite for robust reasoning. We also provide an alternative risk analysis in Appendix B for similar conclusions.

3.3. Takeaways

Our previous analysis from the perspectives of noise (Subsection 3.1) and risk (Subsection 3.2) yields the following

key conclusions about the factors governing the convergence of the optimal CoT length, L_{opt} , in LLM reasoning via RL.

Remark 1. The intrinsic difficulty of a task dictates L_{opt} via stability requirements. Mathematically, complex tasks are characterized by a larger smoothness parameter β (indicating a rugged loss landscape). Per Term (I) in Theorem 3.5, a large β amplifies the stability cost, necessitating lower optimization noise (σ) to prevent the empirical risk from exploding. Consequently, the policy must suppress noise by extending the reasoning process, converging to a longer L_{opt} to ensure precise convergence.

Remark 2. Model capacity is inversely related to the optimal CoT length due to noise regularization. According to Term (II) in Theorem 3.5, higher-capacity models exhibit greater thought dispersion (\mathbb{V}_t), increasing the generalization gap. To mitigate this, they require a higher noise scale σ to mask prompt sensitivities. This necessitates a shorter, more concise L_{opt} to introduce the required stochasticity.

Remark 3. The converged CoT length is independent of the specific RL algorithm used. Our analysis indicates that L_{opt} is an intrinsic property determined by task difficulty and model capacity. The algorithm’s role is more likely to effectively optimize the policy to find this good solution.

Remark 4. The optimization noise scale is inversely correlated with the converged CoT length. Theorem 3.1 shows that higher noise levels incentivize convergence to a shorter L_{opt} , as noisier environments favor more robust, concise reasoning paths that are less susceptible to disruption.

To validate these theoretical claims, the following section presents a series of experiments designed to systematically test each of these four remarks.

4. Experiments

This section presents a series of experiments designed to empirically validate the theoretical insights established in Section 3. We systematically investigate the relationship between the optimal CoT length (L_{opt}) and four key factors. The detailed experimental setup is listed in Appendix D.

Task Difficulty and L_{opt} . To validate Remark 1, we test on tasks of increasing difficulty (GSM8K and five levels of MATH) with Qwen2.5-7B-Base. As shown in Figure 5(a), L_{opt} demonstrates a clear monotonic increase with task complexity. This aligns with Theorem 3.5, as more challenging tasks require a greater reasoning depth. To avoid the high empirical loss from underfitting, the policy learns to generate a correspondingly longer CoT. Additional validations are in Appendix E.

Model Capacity and L_{opt} . To verify Remark 2, we examine models with varying capacities. Figure 5(b) reveals

Why Does Reasoning Length Converge? Unveiling the Underfitting-Overfitting Trade-off in Chain-of-Thought

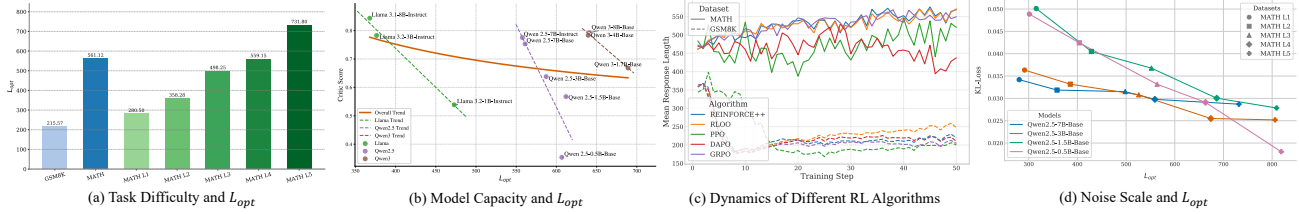


Figure 5. Empirical validation of factors governing optimal CoT length (L_{opt}). (a) **Task difficulty**: L_{opt} increases with task complexity. (b) **Model capacity**: More powerful models converge to a shorter L_{opt} to mitigate overfitting. (c) **RL algorithm**: The converged L_{opt} is largely algorithm-agnostic. (d) **Optimization noise**: L_{opt} is inversely correlated with noise (proxied by KL-Loss).

a distinct negative correlation: within each model family (e.g., Llama 3, Qwen 2.5, and Qwen 3), larger and higher-performing models consistently converge to a shorter L_{opt} . This finding supports our analysis based on Theorem 3.5. Larger models are more prone to overfitting, a risk exacerbated by longer CoTs. Consequently, they learn to produce more concise reasoning to minimize total error by balancing empirical performance with generalization.

RL Algorithm and L_{opt} . To test Remark 3, we compare five different RL algorithms. As shown in Figure 5(c), despite different learning dynamics, all algorithms guide the policy to a similar final L_{opt} for a given task and model, even though the initial dynamics differ. This supports our claim that the RL algorithm primarily facilitates optimization, while the final L_{opt} is an intrinsic property determined by task difficulty and model capacity.

Noise Scale and L_{opt} . Finally, to validate Remark 4, we use the KL-Loss as a proxy for optimization noise. Figure 5(d) shows a clear inverse correlation between the final KL-Loss and L_{opt} . This result substantiates Theorem 3.1, confirming that noisier optimization environments favor shorter CoTs to ensure robust convergence, as longer reasoning paths are more susceptible to disruption.

5. Related Work

Reasoning with LLMs. Prompting techniques have advanced LLM reasoning beyond few-shot learning (Brown et al., 2020). Chain-of-Thought (CoT) prompting elicits its intermediate reasoning steps (Wei et al., 2022b), with methods like Self-Consistency improving robustness (Wang et al., 2022). Other reasoning formats include Program-of-Thought (Chen et al., 2022) and internal thought tokens (Zelikman et al., 2024; Chen et al., 2025a). While theoretical analyses are emerging (Ton et al., 2024), much of these remains empirical and lacks a unifying theoretical foundation.

RL for LLM Reasoning. RL is a key method for test-time scaling, a technique proven to enhance LLM reasoning (Snell et al., 2024; Wu et al., 2024; Chen et al., 2025b). Research in this area follows two main tracks: developing new post-training frameworks like VC-PPO, DAPO, and

VAPO (Yuan et al., 2025; Yu et al., 2025; Yue et al., 2025b), and understanding the fundamental effects of RL. Studies in the latter track investigate RL’s advantages over SFT (Setlur et al., 2025), its impact on knowledge boundaries (Yue et al., 2025a), the role of reward modeling (Shao et al., 2025), and its tendency to amplify pre-trained behaviors (Zhao et al., 2025). The absence of a common theoretical framework, however, can lead to divergent findings.

Optimization and Generalization. A core concept in machine learning optimization is that flatter minima in the loss landscape often lead to better generalization, a principle central to Sharpness-Aware Minimization (SAM) (Keskar et al., 2016). This effect is closely linked to the noise inherent in the optimization process (Smith & Le, 2018). Generalization itself, which measures performance on unseen data, is often analyzed through the powerful lens of information theory. Concepts like entropy and mutual information are used to establish theoretical bounds on the generalization capacity of deep learning models (Russo & Zou, 2019; Xu & Raginsky, 2017) and have recently been applied to analyze synthetic data generation and reasoning errors in LLMs (Gan & Liu, 2024; Ton et al., 2024).

6. Conclusion

In this paper, we introduced CoT-Space, a novel theoretical framework that addresses the critical misalignment between token-level reasoning formulation and the reasoning-level nature of CoT by reframing LLM reasoning as a continuous state optimization problem. This shift in perspective serves as a conceptual bridge, demonstrating that the foundational principles of classical machine learning are not obsolete but can be powerfully revitalized to analyze modern LLM behaviors. By revitalizing classical concepts of noise and risk analysis, we demonstrate that a fundamental trade-off between underfitting (shorter CoTs) and overfitting (longer CoTs) governs the reasoning process. This analysis provides a solid theoretical grounding for the existence of an optimal CoT length, L_{opt} , that minimizes total error. Looking forward, the CoT-Space framework offers a foundation for designing more principled algorithms and advancing our ability to build more reliable AI reasoning systems.

Impact Statement

This paper presents work whose goal is to advance the field of Machine Learning. There are many potential societal consequences of our work, none of which we feel must be specifically highlighted here.

References

- Ahmadian, A., Cremer, C., Gallé, M., Fadaee, M., Kreutzer, J., Pietquin, O., Üstün, A., and Hooker, S. Back to basics: Revisiting reinforce style optimization for learning from human feedback in llms. *arXiv preprint arXiv:2402.14740*, 2024.
- Brown, T., Mann, B., Ryder, N., Subbiah, M., Kaplan, J. D., Dhariwal, P., Neelakantan, A., Shyam, P., Sastry, G., Askell, A., et al. Language models are few-shot learners. *Advances in neural information processing systems*, 33: 1877–1901, 2020.
- Chen, Q., Qin, L., Liu, J., Peng, D., Guan, J., Wang, P., Hu, M., Zhou, Y., Gao, T., and Che, W. Towards reasoning era: A survey of long chain-of-thought for reasoning large language models. *arXiv preprint arXiv:2503.09567*, 2025a.
- Chen, W., Ma, X., Wang, X., and Cohen, W. W. Program of thoughts prompting: Disentangling computation from reasoning for numerical reasoning tasks. *arXiv preprint arXiv:2211.12588*, 2022.
- Chen, Z., Min, Y., Zhang, B., Chen, J., Jiang, J., Cheng, D., Zhao, W. X., Liu, Z., Miao, X., Lu, Y., et al. An empirical study on eliciting and improving r1-like reasoning models. *arXiv preprint arXiv:2503.04548*, 2025b.
- Cobbe, K., Kosaraju, V., Bavarian, M., Chen, M., Jun, H., Kaiser, L., Plappert, M., Tworek, J., Hilton, J., Nakano, R., et al. Training verifiers to solve math word problems. *arXiv preprint arXiv:2110.14168*, 2021.
- Cover, T. M. *Elements of information theory*. John Wiley & Sons, 1999.
- DeepSeek-AI. Deepseek-r1: Incentivizing reasoning capability in llms via reinforcement learning, 2025. URL <https://arxiv.org/abs/2501.12948>.
- Gan, Z. and Liu, Y. Towards a theoretical understanding of synthetic data in llm post-training: A reverse-bottleneck perspective. *arXiv preprint arXiv:2410.01720*, 2024.
- Gan, Z., Liao, Y., and Liu, Y. Rethinking external slow-thinking: From snowball errors to probability of correct reasoning, 2025. URL <https://arxiv.org/abs/2501.15602>.
- Gan, Z., Ren, R., Yao, W., Hu, X., Xu, G., Qian, C., Tang, H., Gong, Z., Yao, X., Tang, P., et al. Beyond the black box: Theory and mechanism of large language models. *arXiv preprint arXiv:2601.02907*, 2026.
- Haenggi, M. On distances in uniformly random networks. *IEEE Transactions on Information Theory*, 51(10):3584–3586, 2005.
- Hendrycks, D., Burns, C., Kadavath, S., Arora, A., Basart, S., Tang, E., Song, D., and Steinhardt, J. Measuring mathematical problem solving with the math dataset. *arXiv preprint arXiv:2103.03874*, 2021.
- Hu, J., Liu, J. K., Xu, H., and Shen, W. Reinforce++: An efficient rlhf algorithm with robustness to both prompt and reward models. *arXiv preprint arXiv:2501.03262*, 2025.
- Ji, Z., Lee, N., Frieske, R., Yu, T., Su, D., Xu, Y., Ishii, E., Bang, Y. J., Madotto, A., and Fung, P. Survey of hallucination in natural language generation. *ACM computing surveys*, 55(12):1–38, 2023.
- Jiang, J., Chen, Z., Min, Y., Chen, J., Cheng, X., Wang, J., Tang, Y., Sun, H., Deng, J., Zhao, W. X., et al. Enhancing llm reasoning with reward-guided tree search. *arXiv preprint arXiv:2411.11694*, 2024.
- Keskar, N. S., Mudigere, D., Nocedal, J., Smelyanskiy, M., and Tang, P. T. P. On large-batch training for deep learning: Generalization gap and sharp minima. *arXiv preprint arXiv:1609.04836*, 2016.
- Li, M., Vitányi, P., et al. *An introduction to Kolmogorov complexity and its applications*, volume 3. Springer, 2008.
- Loshchilov, I. and Hutter, F. Decoupled weight decay regularization. *arXiv preprint arXiv:1711.05101*, 2017.
- McAllester, D. A. Some pac-bayesian theorems. In *Proceedings of the eleventh annual conference on Computational learning theory*, pp. 230–234, 1998.
- Meta. The llama 3 herd of models, 2024. URL <https://arxiv.org/abs/2407.21783>.
- Miyagawa, M. Nearest neighbor distance in three-dimensional space. *Forma*, 33(1):7–11, 2018.
- OpenAI. Learning to reason with llms, 2024. URL <https://openai.com/index/learning-to-reason-with-llms/>. Accessed: September 12, 2024.
- OpenAI. Introducing openai o3 and o4-mini, 2025. URL <https://openai.com/index/introducing-o3-and-o4-mini/>. Accessed: April 16, 2025.

- Qwen, T. Qwq: Reflect deeply on the boundaries of the unknown, November 2024. URL <https://qwenlm.github.io/blog/qwq-32b-preview/>.
- Qwen, T. Qwen2.5 technical report, 2025a. URL <https://arxiv.org/abs/2412.15115>.
- Qwen, T. Qwen3 technical report, 2025b. URL <https://arxiv.org/abs/2505.09388>.
- Razavi, A., Soltangheis, M., Arabzadeh, N., Salamat, S., Zihayat, M., and Bagheri, E. Benchmarking prompt sensitivity in large language models. In *European Conference on Information Retrieval*, pp. 303–313. Springer, 2025.
- Russo, D. and Zou, J. How much does your data exploration overfit? controlling bias via information usage. *IEEE Transactions on Information Theory*, 66(1):302–323, 2019.
- Schulman, J., Wolski, F., Dhariwal, P., Radford, A., and Klimov, O. Proximal policy optimization algorithms. *arXiv preprint arXiv:1707.06347*, 2017.
- Setlur, A., Rajaraman, N., Levine, S., and Kumar, A. Scaling test-time compute without verification or rl is suboptimal. *arXiv preprint arXiv:2502.12118*, 2025.
- Shao, R., Li, S. S., Xin, R., Geng, S., Wang, Y., Oh, S., Du, S. S., Lambert, N., Min, S., Krishna, R., et al. Spurious rewards: Rethinking training signals in rlvr. *arXiv preprint arXiv:2506.10947*, 2025.
- Shao, Z., Wang, P., Zhu, Q., Xu, R., Song, J., Bi, X., Zhang, H., Zhang, M., Li, Y., Wu, Y., et al. Deepseekmath: Pushing the limits of mathematical reasoning in open language models. *arXiv preprint arXiv:2402.03300*, 2024.
- Smith, S. L. and Le, Q. V. A bayesian perspective on generalization and stochastic gradient descent. In *International Conference on Learning Representations*, 2018.
- Snell, C., Lee, J., Xu, K., and Kumar, A. Scaling llm test-time compute optimally can be more effective than scaling model parameters. *arXiv preprint arXiv:2408.03314*, 2024.
- Sui, Y., Chuang, Y.-N., Wang, G., Zhang, J., Zhang, T., Yuan, J., Liu, H., Wen, A., Zhong, S., Chen, H., et al. Stop overthinking: A survey on efficient reasoning for large language models. *arXiv preprint arXiv:2503.16419*, 2025.
- Ton, J.-F., Taufiq, M. F., and Liu, Y. Understanding chain-of-thought in llms through information theory. *arXiv preprint arXiv:2411.11984*, 2024.
- Wan, Z., Feng, X., Wen, M., McAleer, S. M., Wen, Y., Zhang, W., and Wang, J. Alphazero-like tree-search can guide large language model decoding and training. In *International Conference on Machine Learning*, pp. 49890–49920. PMLR, 2024.
- Wang, X., Wei, J., Schuurmans, D., Le, Q., Chi, E., Narang, S., Chowdhery, A., and Zhou, D. Self-consistency improves chain of thought reasoning in language models. *arXiv preprint arXiv:2203.11171*, 2022.
- Wang, Z. and Mao, Y. On the generalization of models trained with SGD: Information-theoretic bounds and implications. In *International Conference on Learning Representations*, 2022. URL <https://openreview.net/forum?id=oWZsQ8o5EA>.
- Wei, J., Tay, Y., Bommasani, R., Raffel, C., Zoph, B., Borgeaud, S., Yogatama, D., Bosma, M., Zhou, D., Metzler, D., et al. Emergent abilities of large language models. *arXiv preprint arXiv:2206.07682*, 2022a.
- Wei, J., Wang, X., Schuurmans, D., Bosma, M., Xia, F., Chi, E., Le, Q. V., Zhou, D., et al. Chain-of-thought prompting elicits reasoning in large language models. *Advances in neural information processing systems*, 35:24824–24837, 2022b.
- Wu, Y., Sun, Z., Li, S., Welleck, S., and Yang, Y. Inference scaling laws: An empirical analysis of compute-optimal inference for problem-solving with language models. *arXiv preprint arXiv:2408.00724*, 2024.
- Xu, A. and Raginsky, M. Information-theoretic analysis of generalization capability of learning algorithms. *Advances in neural information processing systems*, 30, 2017.
- Yao, S., Yu, D., Zhao, J., Shafran, I., Griffiths, T., Cao, Y., and Narasimhan, K. Tree of thoughts: Deliberate problem solving with large language models. *Advances in neural information processing systems*, 36:11809–11822, 2023.
- Yu, Q., Zhang, Z., Zhu, R., Yuan, Y., Zuo, X., Yue, Y., Dai, W., Fan, T., Liu, G., Liu, L., et al. Dapo: An open-source llm reinforcement learning system at scale. *arXiv preprint arXiv:2503.14476*, 2025.
- Yuan, Y., Yue, Y., Zhu, R., Fan, T., and Yan, L. What’s behind ppo’s collapse in long-cot? value optimization holds the secret. *arXiv preprint arXiv:2503.01491*, 2025.
- Yue, Y., Chen, Z., Lu, R., Zhao, A., Wang, Z., Song, S., and Huang, G. Does reinforcement learning really incentivize reasoning capacity in llms beyond the base model? *arXiv preprint arXiv:2504.13837*, 2025a.

- Yue, Y., Yuan, Y., Yu, Q., Zuo, X., Zhu, R., Xu, W., Chen, J., Wang, C., Fan, T., Du, Z., et al. Vapo: Efficient and reliable reinforcement learning for advanced reasoning tasks. *arXiv preprint arXiv:2504.05118*, 2025b.
- Zelikman, E., Harik, G., Shao, Y., Jayasiri, V., Haber, N., and Goodman, N. D. Quiet-star: Language models can teach themselves to think before speaking. *arXiv preprint arXiv:2403.09629*, 2024.
- Zhang, D., Zhoubian, S., Hu, Z., Yue, Y., Dong, Y., and Tang, J. Rest-mcts*: Llm self-training via process reward guided tree search. *Advances in Neural Information Processing Systems*, 37:64735–64772, 2024.
- Zhao, R., Meterez, A., Kakade, S., Pehlevan, C., Jelassi, S., and Malach, E. Echo chamber: RL post-training amplifies behaviors learned in pretraining. *arXiv preprint arXiv:2504.07912*, 2025.
- Zhuo, J., Zhang, S., Fang, X., Duan, H., Lin, D., and Chen, K. Prosa: Assessing and understanding the prompt sensitivity of llms. In *Findings of the Association for Computational Linguistics: EMNLP 2024*, pp. 1950–1976, 2024.

A. Limitations of Token-Level Formulation in Natural Language

Consider a CoT reasoning process comprises multiple conceptual steps $(\xi_1, \xi_2, \dots, \xi_L)$, which naturally reveals two distinct procedural layers:

- (1) **Reasoning-Level:** The strategic planning of abstract reasoning steps $(\xi_1 \rightarrow \xi_L)$.
- (2) **Token-Level:** The tactical realization of specific steps via token generation.

Traditional MDP formulations, however, operate only at the problematic token level, failing to capture the higher-order planning inherent to CoT.

The token-level state space \mathcal{S} is problematic for two reasons. First, it grows exponentially with sequence length ($\mathcal{S}_t = \mathcal{A}^t$), making it too vast to explore effectively during training. Second, the auto-regressive process imposes a discrete and unidirectional topology, $(\forall s_t \in \mathcal{S}_t, \mathcal{T}(s_t, \pi) \in \mathcal{S}_{t+1})$ further complicating analysis. This narrow focus creates a theoretical barrier that obscures the problem’s true nature. To establish a sound foundation, we must therefore transition from a token-level formulation to a reasoning-level perspective.

B. An Alternative Risk Analysis from Information-Theoretic Perspective

Here, we analyze the generalization risk of a policy to provide further theoretical insights, focusing on the upper bounds of reasoning risks. In the context of CoT-Space, risks can be defined similarly to classical ML. The total expected error of a policy π on the true data distribution \mathcal{D} , denoted by $R(\pi) = \mathbb{E}_{q \sim \mathcal{D}}[C(s_q^\pi, q)]$, can be decomposed into two distinct components: $R(\pi) = \hat{R}_n(\pi) + (R(\pi) - \hat{R}_n(\pi))$.

$$R(\pi) = \underbrace{\hat{R}_n(\pi)}_{\text{Empirical Loss (Bias)}} + \underbrace{(R(\pi) - \hat{R}_n(\pi))}_{\text{Generalization Error (Variance)}}. \quad (1)$$

Here, $\hat{R}_n(\pi) = \frac{1}{n} \sum_{i=1}^n C(s_{q_i}^\pi, q_i)$ is the empirical loss (a.k.a. bias) on the training set. $R(\pi) - \hat{R}_n(\pi) = \mathbb{E}_{q \sim \mathcal{D}}[C(s_q^\pi, q)] - \frac{1}{n} \sum_{i=1}^n C(s_{q_i}^\pi, q_i)$ is the reasoning generalization error (a.k.a. virance). In the following parts, we will analyze how each component behaves as a function of the CoT complexity.

B.1. An Upper Bound for Generalization Error: The Overfitting Risk

Given n queries $\{q_i\}_{i=1}^n$ sampled i.i.d. from a distribution \mathcal{D} , and a policy π learned from $\{q_i\}_{i=1}^n$, let’s denote $s_q^\pi = \pi(q)$ as the end reasoning state output by π on query q . The reasoning generalization error of π on \mathcal{D} is defined as: $R(\pi) - \hat{R}_n(\pi) = \mathbb{E}_{q \sim \mathcal{D}}[C(s_q^\pi, q)] - \frac{1}{n} \sum_{i=1}^n C(s_{q_i}^\pi, q_i)$. This error quantifies a policy’s ability to generalize its reasoning to unseen queries, a concept parallel to the generalization error in traditional machine learning theory. By applying classical PAC-Bayesian and information-theoretic results of ML, we can derive an upper bound for the reasoning generalization error.

Theorem B.1. (*Information-theoretical generalization upper bound for LLM reasoning.*) *With CoT-Space defined above, if the policy π is trained on an i.i.d. drawn training set S with size n , the following upper bound for the reasoning generalization error holds:*

$$|\mathbb{E}[R(\pi) - \hat{R}_n(\pi)]| \leq \sqrt{\frac{C_{max}^2 \cdot (\mathbb{E}_{\pi, S}[K]) \cdot \log |\mathcal{A}|}{2n}},$$

where C_{max} is the maximum possible value of the reasoning loss $C(\cdot)$, L is the number of reasoning steps in a CoT data, $|\xi_i|$ is the number of tokens in the i -th reasoning step in a CoT data, $\mathbb{E}[K] \approx \mathbb{E}[L] \cdot \mathbb{E}[|\xi|]$ is the expected total number of tokens in the generated CoT.

A detailed discussion and proof are provided in Appendix C.7. Theorem B.1 explicitly connects the generalization error to the observable, structural properties of the reasoning process. It suggests that overfitting can occur in overlone response length. This provides a direct theoretical basis for regularizing the CoT generation process in RL to improve reasoning generalization.

It is important to acknowledge that standard generalization bounds typically assume i.i.d. data distributions, whereas RL involves non-stationary, on-policy data generation. However, we apply these classical bounds here as a conceptual

proxy to capture the structural relationship between policy complexity (proxied by CoT length L) and generalization risk. This theoretical framing allows us to mechanistically interpret “overthinking” as a form of overfitting, where the policy memorizes complex reasoning paths rather than learning generalizable logic. Developing tighter bounds specifically for the non-stationary RL setting remains a critical direction for future work.

B.2. A Lower Bound for Empirical Loss: The Underfitting Risk

The empirical loss, $\hat{R}_n(\pi)$, measures a policy’s ability to solve the problems it has already encountered. For complex reasoning tasks, a certain minimum number of steps is required for a correct solution. Intuitively, if L is too small, the policy lacks the necessary “thinking space” to solve the queries, even those in the training set. This leads to high empirical loss and underfitting. As L increases, the policy has more capacity to find the correct reasoning path, so the empirical loss $\hat{R}_n(\pi)$ generally decreases.

Building upon this intuition, we can derive a lower bound for the empirical reasoning loss $\hat{R}_n(\pi)$.

Theorem B.2. *With CoT-Space defined above, if the policy π is trained on an i.i.d. drawn training set, the following lower bound for the empirical reasoning risk holds:*

$$\hat{R}_n(\pi) \geq P_\pi(L < L^*) \cdot C_{fail},$$

where L^* is the intrinsic required reasoning depth for the query. Note that L^* is a theoretical property of the problem difficulty and is unobservable in practice. This theorem formalizes the intuition that if a policy generates a CoT shallower (L) than the problem requires (L^*), it is guaranteed to fail (underfit). C_{fail} is the upper bound of the reasoning loss in the failed reasoning results.

A detailed proof is provided in Appendix C.8. Theorem B.2 provides a formal basis for the “underfitting” portion of our trade-off curve. It demonstrates that the empirical loss is directly constrained by the probability that the policy generates a CoT that is too short for the problem’s intrinsic complexity. A policy that tends to produce short CoTs will have a high failure rate on non-trivial problems. Consequently, its empirical loss $\hat{R}_n(\pi)$ is guaranteed to be high. This formalizes why a policy must maintain enough CoT length L to achieve a low empirical loss, thus completing our explanation for the tradeoff in our total error analysis and the existence of an optimal L_{opt} .

C. Proofs

C.1. Proof of Assumption 2.9

In this section, we provide a formal justification for Assumption 2.9. We demonstrate that for any non-trivial semantic concept, the number of valid token-level realizations grows exponentially with the sequence length. We ground this analysis in Kolmogorov Complexity and the combinatorial properties of natural language.

Let \mathcal{A} be the discrete vocabulary of tokens, where $|\mathcal{A}| = V$. The space of all token sequences of length k is \mathcal{A}^k . Let ψ be a specific abstract reasoning step (a semantic concept). We define the Kolmogorov Complexity for natural language as follows:

Definition C.1. (Kolmogorov complexity for natural language.) We define the Kolmogorov Complexity for natural language, denoted as $K(\psi)$, as the length of the shortest possible description (or program) p that can effectively communicate the semantic meaning of ψ in a universal language (Li et al., 2008):

$$K(\psi) = \min_p \{|p| : U(p) \equiv \psi\},$$

where U is a universal Turing machine (or in our context, an ideal language decoder), and \equiv denotes semantic equivalence.

Let $L_{min}(\psi) = K(\psi)$ be the length of the shortest natural language sequence that maps to ψ . Let p_ψ be the shortest realization of the semantic concept ψ where $|p| = L_{min}(\psi)$. We provide the proof for the following lemma which characterizes the exponential growth of semantic equivalence set $\mathcal{V}(p_\psi, k)$:

Lemma C.2. (Exponential growth of semantic equivalence set.) *For a semantic concept ψ with minimal description length L_{min} , the size of its semantic equivalence set $|\mathcal{V}(p_\psi, k)|$ (the number of distinct token sequences of length k that decode to ψ) satisfies:*

$$|\mathcal{V}(\psi, k)| \geq \alpha \cdot c^k,$$

for some constants $\alpha > 0$ and $c > 1$, provided $k \geq L_{min}$.

The proof can be derived from two perspectives. We first consider the combinatorial construction via semantic-preserving operations.

Proof. (Combinatorial construction via semantic-preserving operations.) Let τ_0 be a minimal sequence realizing ψ , such that $|\tau_0| = L_{min}$. We can transform τ_0 into longer sequences without altering its core semantics by applying a set of Semantic-Preserving Operations (SPOs), denoted as $\mathcal{O} = \{op_1, op_2, \dots, op_m\}$. Common SPOs in natural language include:

- **Synonym Replacement:** Replacing a token with a synonym (e.g., “calculate” \rightarrow “compute”).
- **Syntactic Expansion:** Adding non-functional modifiers or filler phrases (e.g., “Therefore” \rightarrow “It can be clearly seen that”).
- **Structural Permutation:** Changing active voice to passive voice, or reordering independent clauses.

Let each operation op_i increase the sequence length by an average of Δl tokens and have a branching factor of b (i.e., there are b different ways to apply operations to increase length). To generate a sequence of target length k starting from τ_0 , we need to apply approximately $j = (k - L_{min})/\Delta l$ operations.

The number of distinct paths to generate a valid sequence of length k is determined by the branching factor b applied j times. Thus, the lower bound on the number of realizations is:

$$|\mathcal{V}(p_\psi, k)| \geq b^j = b^{\frac{k-L_{min}}{\Delta l}}. \quad (2)$$

We can rewrite this term to isolate k :

$$|\mathcal{V}(p_\psi, k)| \geq \left(b^{\frac{1}{\Delta l}}\right)^k \cdot \left(b^{-\frac{L_{min}}{\Delta l}}\right). \quad (3)$$

Let $c = b^{1/\Delta l}$ and $\alpha = b^{-L_{min}/\Delta l}$. Since there are multiple valid synonyms and syntactic structures for any non-trivial concept, $b > 1$, and consequently $c > 1$. Thus, we obtain:

$$|\mathcal{V}(p_\psi, k)| = \Omega(c^k). \quad (4)$$

This finishes the proof. □

Alternatively, we can consider the information capacity of the reasoning process:

Proof. (Information-theoretic perspective.) Let the generation of a natural language token sequence be modeled as a stochastic process $\mathcal{X} = \{X_1, X_2, \dots\}$. The uncertainty of this process is measured by its Entropy Rate, denoted as $H(\mathcal{X})$.

While the theoretical maximum entropy of selecting from a vocabulary \mathcal{A} is $\log_2 |\mathcal{A}|$, natural language is constrained by grammar and logic, resulting in a lower actual entropy. We define the Effective Vocabulary Size, V_{eff} , as the weighted branching factor of the language:

$$V_{eff} = 2^{H(\mathcal{X})}. \quad (5)$$

Physically, V_{eff} represents the average number of plausible next-token choices available to the model at any given step. For any expressive language, $V_{eff} > 1$.

According to the Asymptotic Equipartition Property (AEP) in information theory (Cover, 1999), as the sequence length k increases, the set of valid natural language sequences concentrates in the Typical Set $A_\epsilon^{(k)}$. The size of this set scales as:

$$|A_\epsilon^{(k)}| \approx 2^{k \cdot H(\mathcal{X})} = (V_{eff})^k. \quad (6)$$

Now, consider the subset of sequences that specifically encode the semantic concept ψ . Let $K(\psi)$ denote the minimal information (in bits) required to specify the semantics of ψ . The redundancy available for syntactic variation is the difference between the channel capacity and the semantic payload:

$$R(k) = k \log_2 V_{eff} - K(\psi). \quad (7)$$

This “free information” $R(k)$ allows for variations in style, phrasing, and intermediate derivation steps without altering the final semantic truth. The number of valid realizations N is determined by this redundancy:

$$N \propto 2^{R(k)} = 2^{k \log_2 V_{eff} - K(\psi)} = \frac{(V_{eff})^k}{2^{K(\psi)}}. \quad (8)$$

Since $K(\psi)$ is a constant intrinsic to the concept, and $V_{eff} > 1$ for any non-trivial language model, the term $(V_{eff})^k$ dominates. Consequently, the number of semantically equivalent realizations grows exponentially with the sequence length k , i.e.:

$$|\mathcal{V}(p_\psi, k)| = \Omega(c^k). \quad (9)$$

This finishes the proof. □

By simply applying Lemma C.2, we can directly derive Assumption 2.9.

C.2. Proof of Lemma 2.10

Proof. We begin with the definition of the number of realizations for a complete reasoning process.

Definition C.3. (Number of realizations.) For a complete reasoning trajectory of L steps, $(\xi_1, \xi_2, \dots, \xi_L)$, its total number of token-level realizations, N_{realize} , is the size of the Cartesian product of the semantic equivalence sets for each step.

$$N_{\text{realize}}(\xi_1, \dots, \xi_L) = \prod_{l=1}^L |\mathcal{V}(\xi_l, k_l)|.$$

Consider a single, fixed reasoning-level path (ξ_1, \dots, ξ_L) , where each step ξ_l is realized by an average of k tokens. By Assumption 2.9, the number of token-level realizations for this single path, N_{realize}^K , is bounded below:

$$N_{\text{realize}}^K \geq \prod_{l=1}^L c^{k_l} = c^{\sum_{l=1}^L k_l} = c^{kL} = c^K. \quad (10)$$

This shows that the number of token-level trajectories corresponding to even a single reasoning path grows exponentially with the total number of tokens, denoted as $K = kL$.

Next, we consider the total number of distinct, valid reasoning states, $|\mathcal{S}_{\text{reasoning}}^{(K)}|$. For complex problems, given a total token amount K , the valid reasoning paths can be realized in distinct lengths that are no longer than K , which means $|\mathcal{S}_{\text{reasoning}}^{(K)}| = \sum_{K' \leq K} N_{\text{realize}}^{K'}$. According to Equation (10), the number of realizations is bounded by an exponential term of the total number of tokens K , thus $|\mathcal{S}_{\text{reasoning}}^{(K)}|$ is of the same order with N_{realize}^K .

$$|\mathcal{S}_{\text{reasoning}}^{(K)}| = \Theta(c^K). \quad (11)$$

From Definition 2.8, the reasoning state density $\rho(K)$ is thus:

$$\rho(K) = \frac{|\mathcal{S}_{\text{reasoning}}^{(K)}|}{|\mathcal{V}_{\text{semantic}}|} = \Theta(c^K). \quad (12)$$

Assuming the semantic volume $\mathcal{V}_{\text{semantic}}$ for a given problem domain is fixed, the state density $\rho(K)$ thus grows exponentially with K .

Finally, we connect high density to the expected distance between adjacent points with the following lemma.

Lemma C.4. (Nearest neighbor distance). *Let points be distributed in a d -dimensional Euclidean space \mathbb{R}^d according to a homogeneous Poisson point process with density ρ . The expected distance to the k -th nearest neighbor, denoted by $\mathbb{E}[R_k]$, is given by*

$$\mathbb{E}[R_k] = \frac{1}{(k-1)!} \left(\frac{1}{\rho C_d} \right)^{1/d} \Gamma\left(k + \frac{1}{d}\right),$$

where $C_d = \frac{\pi^{d/2}}{\Gamma(\frac{d}{2}+1)}$ is the volume of a unit d -dimensional ball and $\Gamma(\cdot)$ is the Gamma function.

The proof is provided in Appendix C.3. Lemma C.4 implies the relation between the density and the expected distance of the points in a space. By only considering the nearest adjacent points, in a D -dimensional space, the expected distance $\mathbb{E}[\text{dist}_{s_i \triangleright s_j}(s_i, s_j)]$ between adjacent nearest neighbor points s_i, s_j is inversely related to the density, approximately scaling as:

$$\mathbb{E}_{s_i \triangleright s_j}[\text{dist}(s_i, s_j)] \propto \rho^{-1/D}. \quad (13)$$

Since $\rho(K)$ grows exponentially, it follows that:

$$\lim_{K \rightarrow \infty} \mathbb{E}_{s_i \triangleright s_j}[\text{dist}(s_i, s_j)] = 0. \quad (14)$$

When the expected distance between states approaches zero, it implies that for any state and any direction, another valid state can be found within an infinitesimally small neighborhood. This is the defining characteristic of a continuous space or manifold. Therefore, as the reasoning token amount K increases, the discrete CoT-Space increasingly resembles a continuum, which validates the application of continuous optimization tools for its analysis.

This finishes the proof. □

C.3. Proof of Lemma C.4

Proof. The proof is built upon Haenggi (2005) and Miyagawa (2018).

First, we derive the probability density function, $f_k(r)$, for the distance to the k -th nearest neighbor. The cumulative distribution function (CDF), $F_k(r)$, is the probability that a d -dimensional ball B_r of radius r contains at least k points. The volume of this ball is $V_d(r) = C_d r^d$.

The number of points X in a region of volume V follows a Poisson distribution with mean ρV :

$$P(X = x) = \frac{(\rho V)^x}{x!} e^{-\rho V}. \quad (15)$$

The CDF is therefore 1 minus the probability of finding fewer than k points in the ball B_r :

$$F_k(r) = P(\text{points in } B_r \geq k) = 1 - \sum_{x=0}^{k-1} P(X = x) = 1 - e^{-\rho C_d r^d} \sum_{x=0}^{k-1} \frac{(\rho C_d r^d)^x}{x!}. \quad (16)$$

The PDF is the derivative of the CDF with respect to r :

$$f_k(r) = \frac{d}{dr} F_k(r) = -\frac{d}{dr} \left(e^{-\rho C_d r^d} \sum_{x=0}^{k-1} \frac{(\rho C_d r^d)^x}{x!} \right). \quad (17)$$

Using the product rule, the derivative simplifies due to a telescoping sum, yielding:

$$f_k(r) = \frac{d(\rho C_d)^k r^{dk-1}}{(k-1)!} e^{-\rho C_d r^d}. \quad (18)$$

The expected value $\mathbb{E}[R_k]$ is defined as the integral of r times its PDF over its domain:

$$\mathbb{E}[R_k] = \int_0^\infty r \cdot f_k(r) dr. \quad (19)$$

Substituting the PDF we derived:

$$\mathbb{E}[R_k] = \int_0^\infty r \cdot \left(\frac{d(\rho C_d)^k r^{dk-1}}{(k-1)!} e^{-\rho C_d r^d} \right) dr. \quad (20)$$

We combine the terms involving r and move the constants outside the integral:

$$\mathbb{E}[R_k] = \frac{d(\rho C_d)^k}{(k-1)!} \int_0^\infty r^{dk} e^{-\rho C_d r^d} dr. \quad (21)$$

To solve the integral, we perform a change of variables. Let $t = \rho C_d r^d$. This implies:

$$r = \left(\frac{t}{\rho C_d} \right)^{1/d} \quad \text{and} \quad dt = d\rho C_d r^{d-1} dr. \quad (22)$$

The integral becomes:

$$\begin{aligned} \int_0^\infty r^{dk} e^{-\rho C_d r^d} dr &= \int_0^\infty \left(\frac{t}{\rho C_d} \right)^k e^{-t} \frac{dt}{d\rho C_d r^{d-1}} \\ &= \int_0^\infty \left(\frac{t}{\rho C_d} \right)^k e^{-t} \frac{dt}{d\rho C_d (t/(\rho C_d))^{(d-1)/d}} \\ &= \frac{1}{d(\rho C_d)^{k+1-(d-1)/d}} \int_0^\infty t^{k-(d-1)/d} e^{-t} dt \\ &= \frac{1}{d(\rho C_d)^{k+1/d}} \int_0^\infty t^{(k+1/d)-1} e^{-t} dt. \end{aligned} \quad (23)$$

The remaining integral is the definition of the Gamma function, $\Gamma(k+1/d)$. Thus:

$$\int_0^\infty r^{dk} e^{-\rho C_d r^d} dr = \frac{\Gamma(k+1/d)}{d(\rho C_d)^{k+1/d}}. \quad (24)$$

Substituting this result back into the expression for $\mathbb{E}[R_k]$:

$$\mathbb{E}[R_k] = \frac{d(\rho C_d)^k}{(k-1)!} \left(\frac{\Gamma(k+1/d)}{d(\rho C_d)^{k+1/d}} \right). \quad (25)$$

The terms d and $(\rho C_d)^k$ cancel out, leaving:

$$\mathbb{E}[R_k] = \frac{1}{(k-1)!} \frac{\Gamma(k+1/d)}{(\rho C_d)^{1/d}}. \quad (26)$$

Which can be written as the final result:

$$\mathbb{E}[R_k] = \frac{1}{(k-1)!} \left(\frac{1}{\rho C_d} \right)^{1/d} \Gamma\left(k + \frac{1}{d}\right). \quad (27)$$

This finishes the proof. □

C.4. Proof of Theorem 2.12

Our goal is to show that both error components converge to zero as the reasoning state density $\rho(K)$ increases. Consider a D -dimensional semantic space. This analysis is predicated on a reasonable assumption about the locality of a single reasoning step.

Assumption C.5. (Bounded step optimization). Any single reasoning step corresponds to a transition in the semantic space with an effective maximum radius R_{\max} and a minimum radius R_{\min} . Thus, from a state s , the set of all possible subsequent states is contained within the region between two concentric D -dimensional hyperspheres centered at s with radii R_{\min} and R_{\max} . This region can be denoted as $B_R(s)$.

Following Assumption C.5, we continue to use the following definition to characterize the distribution structure of state points in the semantic space.

Definition C.6. (Maximal void.) The maximal void $B_R^{\text{hole}}(s)$ is defined as the largest void hypersphere region within the bounded step radius. Formally, it is the largest hypersphere subspace of $B_R(s)$ that does not contain any state points:

$$B_R^{\text{hole}}(s) = \arg \max_B \{r(B) \mid B \subseteq B_R(s) \text{ and } B \cap \mathcal{S} = \emptyset\},$$

where $r(\cdot)$ is the radius of a ball and \mathcal{S} is the reasoning state space.

Let R_{hole} be the radius of $B_R^{\text{hole}}(s)$. We further show the relationship between R_{hole} and the reasoning state density ρ .

Lemma C.7. (Maximal void radius and reasoning state density.) In a D -dimensional semantic space, the radius of the maximal void R_{hole} and the density of reasoning state points $\rho(K)$ have the following relationship:

$$R_{\text{hole}} = \mathcal{O}\left(\rho(K)^{-\frac{1}{D}}\right).$$

Proof. The proof relies on the connection between the average nearest-neighbor distance and the scale of the largest voids in a spatial point process.

As established in Lemma 2.10, which builds upon the theory of spatial point processes (Lemma C.4), the expected distance between adjacent reasoning states in a D -dimensional semantic space is inversely related to the state density $\rho(K)$:

$$\mathbb{E}_{s_i \bowtie s_j} [\text{dist}(s_i, s_j)] \propto \rho(K)^{-1/D}. \quad (28)$$

The radius of the maximal void, R_{hole} , represents the largest possible distance from a point within that void to the nearest available reasoning state. It can thus be understood as a measure of the worst-case nearest-neighbor distance in a local region.

In the study of stochastic geometry, for a homogeneous point process, the distribution of nearest-neighbor distances is concentrated around its mean. Consequently, the scaling of the maximal values is of the same order as the scaling of the expected value.

Given that the expected distance is proportional to $\rho(K)^{-1/D}$, it follows that the maximal void radius, representing the worst-case local distance, must adhere to the same scaling law. Therefore, we can conclude that:

$$R_{\text{hole}} = \mathcal{O}\left(\rho(K)^{-\frac{1}{D}}\right). \quad (29)$$

This finishes the proof. □

With Lemma C.7, we then commence to analyze the convergence of the two continuum errors, respectively.

Analysis of the Angular Error $\epsilon_A(s)$

The angular error measures the difference in direction between discrete steps and continuous steps. Building upon the previous discussion, we can bound the angular error by the following result.

Lemma C.8. (Convergence of the Angular Error). The expected angular error $\mathbb{E}[\epsilon_A(s)]$ is bounded above by a function that is inversely related to the reasoning state density $\rho(K)$:

$$\mathbb{E}[\epsilon_A(s)] \leq \mathcal{O}\left(\rho(K)^{-\frac{1}{D}}\right).$$

Proof. The angular error $\epsilon_A(s)$ is defined as the angle between the ideal step vector \vec{v}_{ideal} and the best achievable discrete step vector \vec{v}_{real} . This error is determined by the directional sparsity of available states in the semantic space.

The worst-case error occurs when the ideal vector \vec{v}_{ideal} points directly towards the center of the maximal void, $B_R^{\text{hole}}(s)$, within the local neighborhood $B_R(s)$. Let the radius of this maximal void be R_{hole} . The ideal target state $p_{\text{ideal}} = s + \vec{v}_{\text{ideal}}$ is at the center of this void.

By definition, the best achievable subsequent state, s_j^* , must lie on or outside the boundary of this void. The vector difference $s_j^* - p_{\text{ideal}}$ represents the deviation from the ideal target.

Let's consider the triangle formed by the points s (current state), p_{ideal} (ideal target), and s_j^* (best achievable state). The angular error $\epsilon_A(s)$ is the angle at vertex s . Using the small-angle approximation for sine, which is valid as the space becomes dense, we can bound the angle:

$$\epsilon_A(s) \approx \sin(\epsilon_A(s)) \approx \frac{\|s_j^* - p_{\text{ideal}}\|}{\|\vec{v}_{\text{real}}\|} \leq \frac{\|s_j^* - p_{\text{ideal}}\|}{R_{\text{min}}}. \quad (30)$$

In the worst-case scenario, the distance from the ideal point to the best real point $\|s_j^* - p_{\text{ideal}}\|$ is bounded by the properties of the void. This distance is on the order of the void's radius, R_{hole} . Since the step size $\|\vec{v}_{\text{real}}\|$ is bounded and non-zero, the angular error is directly proportional to the radius of the maximal void:

$$\epsilon_A(s) = \mathcal{O}(R_{\text{hole}}). \quad (31)$$

Taking the expectation over all possible configurations of the state space, we have:

$$\mathbb{E}[\epsilon_A(s)] = \mathcal{O}(\mathbb{E}[R_{\text{hole}}]). \quad (32)$$

By combining this with Lemma C.7, we establish the bound on the expected angular error:

$$\mathbb{E}[\epsilon_A(s)] \leq \mathcal{O}(\rho(K)^{-\frac{1}{D}}). \quad (33)$$

As established in Lemma 2.10, the reasoning state density $\rho(K)$ grows exponentially with the total reasoning token amount K . Consequently, as $K \rightarrow \infty$, $\rho(K) \rightarrow \infty$, and thus $\lim_{K \rightarrow \infty} \mathbb{E}[\epsilon_A(s)] = 0$. This demonstrates that the direction of the best discrete step converges to the direction of the ideal continuous gradient.

This finishes the proof. □

Analysis of the Magnitude Error $\epsilon_M(s)$

The magnitude error quantifies how well the length of the discrete step matches the length of the ideal step. This insight provides a direct way to bound this error.

Lemma C.9. (Convergence of the Magnitude Error). *The expected magnitude error $\mathbb{E}[\epsilon_M(s)]$ is also bounded above by a function that is inversely related to the reasoning state density $\rho(K)$:*

$$\mathbb{E}[\epsilon_M(s)] \leq \mathcal{O}\left(\rho(K)^{-\frac{1}{D}}\right).$$

Proof. By the reverse triangle inequality, the magnitude error is bounded by the norm of the vector difference:

$$\epsilon_M(s) = \left| \|\vec{v}_{\text{real}}\| - \|\vec{v}_{\text{ideal}}\| \right| \leq \|\vec{v}_{\text{real}} - \vec{v}_{\text{ideal}}\|. \quad (34)$$

Let $p_{\text{ideal}} = s + \vec{v}_{\text{ideal}}$ be the ideal target state. The best achievable state s_j^* is the valid state closest to p_{ideal} . The vector difference is then $\|(s_j^* - s) - (p_{\text{ideal}} - s)\| = \|s_j^* - p_{\text{ideal}}\|$.

In the worst-case scenario, the ideal target p_{ideal} falls within the largest void. The closest available state s_j^* must lie on or outside the boundary of this void. The distance between any point inside a hypersphere and its boundary is at most its diameter, $2R_{\text{hole}}$. Therefore, the distance between the ideal target and the best real state is bounded:

$$\|s_j^* - p_{\text{ideal}}\| \leq 2R_{\text{hole}}. \quad (35)$$

Combining these steps, we get a bound for the magnitude error:

$$\epsilon_M(s) \leq 2R_{\text{hole}}. \quad (36)$$

Taking the expectation and applying Lemma C.7, we find that the expected magnitude error is bounded by the same scaling law as the angular error:

$$\mathbb{E}[\epsilon_M(s)] \leq 2\mathbb{E}[R_{\text{hole}}] = \mathcal{O}\left(\rho(K)^{-1/D}\right). \quad (37)$$

As $K \rightarrow \infty$, $\rho(K) \rightarrow \infty$, and thus $\lim_{K \rightarrow \infty} \mathbb{E}[\epsilon_M(s)] = 0$.

This finishes the proof. □

C.5. Proof of Theorem 3.1

Proof. As previously established, when viewed from a reasoning-level perspective, the reasoning space can be considered approximately continuous, i.e., $s_o \in \mathcal{S}$ where \mathcal{S} is a continuous space. The state is then optimized continuously based on the policy and reasoning loss. This perspective enables us to analyze the reasoning process through a loss-reduction lens.

For an L -step CoT reasoning process, this can be viewed as an L -step optimization based on the gradient of the reasoning loss. A single step of this optimization can be written as:

$$\Delta s = -\frac{1}{L} \frac{d}{ds} \hat{C}, \quad (38)$$

where \hat{C} is a noisy estimation of the reasoning loss, influenced by the policy and random sampling. We assume that \hat{C} is a random variable with expectation C . Here, L represents the total reasoning steps, or the CoT length.

Despite the above gradient descent formulation, this optimization process can also be modeled as a stochastic differential equation (SDE) with L steps:

$$\frac{ds}{dt} = -\frac{dC}{ds} + \zeta(t), \quad (39)$$

where $\zeta(t)$ is the noise term and $t = 1, \dots, L$.

Equations (38) and (39) formulate the optimization process of CoT reasoning from the gradient update and SDE perspective, respectively. By combining the two equations related to noise, we can thus obtain the relationship between noise scale and CoT length, as shown in Theorem 3.1. The detailed derivation of this result is provided below.

To bridge the discrete reasoning update with the continuous SDE model, we equate the variance induced by the noise term in both frameworks over a single reasoning step.

First, we analyze the noise in the discrete one-step reasoning update from Equation (38):

$$\Delta s = -\frac{1}{L} \left(\frac{dC}{ds} + \left(\frac{d\hat{C}}{ds} - \frac{dC}{ds} \right) \right). \quad (40)$$

The noise originates from the estimation error, which we define as $\alpha = \left(\frac{d\hat{C}}{ds} - \frac{dC}{ds} \right)$. We assume this error has a variance $\langle \alpha^2 \rangle = F(s)$, where $F(s)$ is a function characterizing the magnitude of the reasoning loss estimation error at state s . The variance of the full noise term in the discrete update is therefore:

$$\left\langle \left(-\frac{1}{L} \alpha \right)^2 \right\rangle = \frac{1}{L^2} \langle \alpha^2 \rangle = \frac{F(s)}{L^2}. \quad (41)$$

Next, we analyze the noise from the SDE model proposed in Equation (39).

We assume the noise term $\zeta(t)$ is white noise with the statistical properties: $\langle \zeta(t) \rangle = 0$ and autocorrelation $\langle \zeta(t)\zeta(t') \rangle = \sigma F(s) \delta(t - t')$, where g is the noise scale, $F(s)$ is a function characterizing the magnitude of the reasoning loss estimation error at state s , where σ is the noise scale. To find the variance over a discrete step, we integrate the SDE over a time interval $\Delta t = 1/L$:

$$\Delta s = \int_0^{1/L} \left(-\frac{dC}{ds} + \zeta(t) \right) dt = -\frac{1}{L} \frac{dC}{ds} + \int_0^{1/L} \zeta(t) dt. \quad (42)$$

The variance of the noise component of this update is:

$$\left\langle \left(\int_0^{1/L} \zeta(t) dt \right)^2 \right\rangle = \int_0^{1/L} \int_0^{1/L} \langle \zeta(t)\zeta(t') \rangle dt' dt = \int_0^{1/L} \int_0^{1/L} \sigma F(s) \delta(t-t') dt' dt = \frac{\sigma F(s)}{L}. \quad (43)$$

By equating the variance from the discrete update (Eq. 41) and the SDE model (Eq. 43), we can solve for the noise scale σ :

$$\frac{F(s)}{L^2} = \frac{\sigma F(s)}{L}. \quad (44)$$

Solving for g , we find:

$$\sigma = \frac{1}{L}. \quad (45)$$

This result shows that the noise scale g in our CoT-Space SDE model is inversely proportional to the CoT length L .

This finishes the proof. \square

C.6. Proof of Theorem 3.5

Proof. We begin with the necessary assumption for our proof.

Assumption C.10. (Simplified additive noise.) Let $\Delta_t = s_t - s_t^*$ be the deviation of the stochastic trajectory from the deterministic baseline at step t . The dynamics of this deviation are strictly given by

$$\Delta_t = \Delta_{t-1} - \eta[\nabla C(s_{t-1}, q) - \nabla C(s_{t-1}^*, q)] + \sigma \zeta_t. \quad (46)$$

For the purpose of analyzing the raw exploration capacity (dispersion) provided by the noise term, we adopt the Simplified Additive Noise Assumption. We assume that for sufficiently small steps η or within local regions where the gradient field is approximately constant (i.e., $\nabla C(s) \approx \nabla C(s^*)$), the contractive or expansive effects of the drift term difference are second-order compared to the diffusion term. Under this assumption, the deviation dynamics simplify to a random walk:

$$\Delta_t \approx \Delta_{t-1} + \sigma \zeta_t. \quad (47)$$

Consequently, the accumulated deviation at step T , denoted as $\Delta_T = s_T - s_T^*$, follows a centered Gaussian distribution with variance scaling linearly with the path length:

$$\Delta_T \sim \mathcal{N}(0, T\sigma^2 I_d). \quad (48)$$

This assumption allows us to explicitly characterize the ‘‘search radius’’ of the reasoning process as a function of the noise scale σ and chain length T .

We now state our main theorem, which bounds the expected population risk $R_{pop} \triangleq \mathbb{E}_{q,\zeta}[C(s_T, q)]$ in terms of the noise scale σ .

We decompose the population risk into the empirical risk R_{emp} and the generalization gap: $R_{pop} \leq R_{emp} + |R_{pop} - R_{emp}|$, where $R_{emp}(s) \triangleq \frac{1}{n} \sum_{i=1}^n C(s, q_i)$. We analyze the impact of noise σ on each term under the expectation form separately.

$$\underbrace{\mathbb{E}_{q,\zeta}[R_{pop}(s_T)]}_{\text{Total Expected Risk}} = \underbrace{\mathbb{E}_{q,\zeta}[R_{emp}(s_T)]}_{\text{Expected Empirical Risk}} + \underbrace{\mathbb{E}_{q,\zeta}[R_{pop}(s_T) - R_{emp}(s_T)]}_{\text{Expected Generalization Gap}} \quad (49)$$

We first consider bounding the empirical risk $\mathbb{E}_{q,\zeta}[R_{emp}(s_T)]$.

Let s_T^* denote the deterministic reasoning outcome in the T -th step (where $\sigma = 0$) and s_T be the stochastic outcome. The accumulated noise $\Delta_T = s_T - s_T^*$ follows $\Delta_T \sim \mathcal{N}(0, T\sigma^2 I_d)$ under a simplified additive noise assumption. Performing a second-order Taylor expansion of the loss around s_T^* :

$$\mathbb{E}[R_{emp}(s_T)] = \mathbb{E}[R_{emp}(s_T^* + \Delta_T)] \approx R_{emp}(s_T^*) + \mathbb{E}[\nabla R_{emp}(s_T^*)^\top \Delta_T] + \frac{1}{2} \mathbb{E}[\Delta_T^\top \mathbf{H}_{emp}(s_T^*) \Delta_T], \quad (50)$$

where $\mathbf{H}_{emp}(s) = \nabla^2 R_{emp}(s) = \nabla^2 \left(\frac{1}{N} \sum_{i=1}^N C(s, q_i) \right)$.

Due to the zero mean of the noise, the first-order term vanishes to zero:

$$\mathbb{E}[\nabla R_{emp}(s_T^*)^\top \Delta_T] = 0. \quad (51)$$

For the second-order term, we have:

$$\begin{aligned} \mathbb{E}[\Delta_T^\top \mathbf{H}_{emp} \Delta_T] &= \mathbb{E}[\text{Tr}(\Delta_T^\top \mathbf{H}_{emp} \Delta_T)] \\ &= \mathbb{E}[\text{Tr}(\mathbf{H}_{emp} \Delta_T \Delta_T^\top)] \\ &= \text{Tr}(\mathbf{H}_{emp} \cdot \mathbb{E}[\Delta_T \Delta_T^\top]). \end{aligned} \quad (52)$$

Recall that $\Delta_T \sim \mathcal{N}(0, T\sigma^2 I_d)$, we have:

$$\mathbb{E}[\Delta_T \Delta_T^\top] = T\sigma^2 I_d. \quad (53)$$

By the definition,

$$\mathbf{H}_{emp}(s) = \nabla^2 R_{emp}(s) = \nabla^2 \left(\frac{1}{n} \sum_{i=1}^n C(s, q_i) \right) = \frac{1}{n} \sum_{i=1}^n \nabla^2 C(s, q_i) \triangleq \frac{1}{n} \sum_{i=1}^n \mathbf{H}_i(s). \quad (54)$$

Using the β -smoothness condition, $\text{Tr}(\mathbf{H}_i(s_T^*)) \leq d\beta$, thus:

$$\begin{aligned} \text{Tr}(\mathbf{H}_{emp}) &= \text{Tr} \left(\frac{1}{n} \sum_{i=1}^n \mathbf{H}_i \right) = \frac{1}{n} \sum_{i=1}^n \text{Tr}(\mathbf{H}_i) \\ &\leq \frac{1}{n} \sum_{i=1}^n (d\beta) = \frac{1}{n} \cdot n \cdot (d\beta) = d\beta. \end{aligned} \quad (55)$$

Thus, the expected empirical risk increases by at most $\frac{\beta T \sigma^2 d}{2}$. Let $T = L$, this constitutes Term (I):

$$\mathbb{E}[R_{emp}(s_L)] \leq R_{emp}(s_L^*) + \frac{\beta L \sigma^2 d}{2}. \quad (56)$$

This term represents the Optimization Drift: higher noise requires the solution to lie in a flatter region of the loss landscape to maintain accuracy.

We subsequently consider bounding the generalization gap.

Following the information-theoretic framework (Xu & Raginsky, 2017), the generalization gap is bounded by the mutual information between the input query data Q and the final reasoning state s_L : $\mathbb{E}|R_{pop} - R_{emp}| \leq \sqrt{\frac{2\Gamma^2}{n} I(s_L; Q)}$. By the data processing inequality and the chain rule, $I(s_T; Q) \leq \sum_{t=1}^L I(s_t; Q | s_{t-1})$. We invoke Lemma 4 from Wang & Mao (2022), which provides a tight bound for additive Gaussian noise channels:

Lemma C.11. (Upper bound for additive Gaussian noise channels (Wang & Mao, 2022).) *Let random variables X, Y and Δ be independent of $N \sim \mathcal{N}(0, I_d)$. Then for any $\sigma > 0$, any \mathbb{R}^d -valued function f , and any random variable $\Omega \in \mathbb{R}^d$ that is a function of Y , we have*

$$I(f(Y + \Delta, X) + \sigma N; X | Y) \leq \frac{d}{2} \mathbb{E} \left[\log \left(\frac{\mathbb{E} [\|f(Y + \Delta, X) - \Omega\|^2]}{d\sigma^2} + 1 \right) \right]. \quad (57)$$

For a step $s_t = s_{t-1} - \eta \nabla C(s_{t-1}, q) + \sigma \zeta_t$, by mapping the query data Q to X , the previous state s_{t-1} to Y , and the drift term $-\eta \nabla C(s_{t-1}, Q)$ to the function $f(Y, X)$, we obtain:

$$\begin{aligned}
 I(s_t; Q|s_{t-1}) &\leq \frac{d}{2} \log \left(1 + \frac{\mathbb{E}_Q[\| -\eta \nabla C(s_{t-1}, Q) - \mathbb{E}[-\eta \nabla C]\|^2]}{d\sigma^2} \right) \\
 &= \frac{d}{2} \log \left(1 + \frac{\eta^2 \mathbb{V}_t(s_{t-1})}{d\sigma^2} \right),
 \end{aligned} \tag{58}$$

Summing over $t = 1 \dots L$ yields Term (II):

$$\mathbb{E}|R_{pop} - R_{emp}| \leq \sqrt{\frac{2\Gamma^2}{n} \sum_{t=1}^L \frac{d}{2} \log \left(1 + \frac{\eta^2 \mathbb{E}[\mathbb{V}_t(s_{t-1})]}{d\sigma^2} \right)}. \tag{59}$$

This term is a decreasing function of σ , reflecting that noise masks the specific details of the input prompt, thereby preventing the reasoning trajectory from overfitting to prompt-specific shortcuts.

Combining Equations (56) and (59), this finishes the proof. □

C.7. Proof and Analysis of Theorem B.1

To derive an upper bound for the reasoning generalization error, we can first simply adapt the PAC-Bayes framework, which provides a powerful link between generalization, policy complexity, and data volume. For our analysis within CoT-Space, we establish the following components:

- **Hypothesis Space \mathcal{H} :** The space of all possible reasoning policies, denoted by \mathcal{H} . Our learned policy $\pi \in \mathcal{H}$.
- **Prior Distribution P :** A distribution over the policy space \mathcal{H} reflecting our initial beliefs about which policies are "good," often favoring simpler ones.
- **Posterior Distribution Q :** A distribution over \mathcal{H} that is learned from the training data queries $\{q_i\}_{i=1}^n$, concentrating on policies that perform well on that data.

By applying the PAC-Bayes theorem (McAllester, 1998), we obtain a bound on the expected true loss which, when rearranged, yields an upper bound on the expected generalization error.

Theorem C.12. (PAC-Bayesian generalization upper bound for LLM reasoning.) *With CoT-Space defined above, the policy π is trained on an i.i.d. drawn training set with size n , by assuming the reasoning loss is bounded in $[0, 1]$, for any prior P , with probability at least $1 - \delta$, the following holds for all posterior Q :*

$$\mathbb{E}_{\pi \sim Q}[R(\pi) - \hat{R}_n(\pi)] \leq \sqrt{\frac{\text{KL}(Q||P) + \ln \frac{2n}{\delta}}{2n}},$$

where $\text{KL}(Q||P) = \mathbb{E}_{\pi \sim Q}[\ln \frac{Q(\pi)}{P(\pi)}]$ is the Kullback-Leibler (KL) divergence between the posterior and prior distributions.

Proof. Let's denote the true reasoning loss of a policy π as $R(\pi) = \mathbb{E}_{q \sim \mathcal{D}}[C(s_q^\pi, q)]$ and the empirical reasoning loss as $\hat{R}_n(\pi) = \frac{1}{n} \sum_{i=1}^n C(s_{q_i}^\pi, q_i)$. The reasoning generalization error for a specific policy π is $R(\pi) - \hat{R}_n(\pi)$. We aim to bound this gap.

The PAC-Bayes theorem provides a bound on the expected true loss for policies drawn from the posterior Q . A standard version of the theorem is often presented as follows.

Lemma C.13. (PAC-Bayes generalization upper bound (McAllester, 1998).) *For any loss function bounded in $[0, 1]$, for any prior P , with probability at least $1 - \delta$ over the draw of the training set $\{q_i\}_{i=1}^n$, the following holds for all posterior distributions Q :*

$$\mathbb{E}_{\pi \sim Q}[R(\pi)] \leq \mathbb{E}_{\pi \sim Q}[\hat{R}_n(\pi)] + \sqrt{\frac{\text{KL}(Q||P) + \ln \frac{2n}{\delta}}{2n}},$$

where $\text{KL}(Q||P) = \mathbb{E}_{\pi \sim Q}[\ln \frac{Q(\pi)}{P(\pi)}]$ is the Kullback-Leibler (KL) divergence between the posterior and prior distributions.

Let’s adapt Lemma C.13 to our framework. We first need to normalize our reasoning loss $C(\cdot, \cdot)$ to be in $[0, 1]$. Assuming there is a maximum possible loss C_{max} , we can define a normalized loss $C'(\cdot, \cdot) = C(\cdot, \cdot)/C_{max}$. The bound then applies to the normalized losses $R'(\pi)$ and $\hat{R}'_n(\pi)$. For simplicity of notation, let’s assume $C(\cdot, \cdot)$ is already normalized in $[0, 1]$.

This finishes the proof. □

The bound has a clear information-theoretic meaning, which aligns with the goal of understanding reasoning phenomena:

Complexity Term ($\text{KL}(Q||P)$): The KL divergence term measures the information gain in moving from our prior belief P to our posterior belief Q after seeing the data. It quantifies the complexity of the learned policy distribution. If Q is very different from P (i.e., $\text{KL}(Q||P)$ is large), it means we had to learn a great deal from the training data to find a good policy. This is analogous to overfitting or memorizing the training set. The bound becomes looser (larger), penalizing this complexity and suggesting a higher risk of poor generalization. If Q remains close to P ($\text{KL}(Q||P)$ is small), it implies the learned policy did not stray far from our initial bias towards simpler policies. The bound is tighter, suggesting better generalization.

Data Term ($\frac{1}{n}$): The bound depends on the number of training queries n . As n increases, the term under the square root decreases, making the bound tighter. This confirms the intuition that having more data leads to better generalization and reduces the gap between training and test performance.

In conclusion, this PAC-Bayes bound formalizes the trade-off in learning a reasoning policy. To achieve good generalization, a policy π must not only achieve a low empirical reasoning loss $\hat{R}_n(\pi)$ on the queries it has seen, but it must also remain simple in an information-theoretic sense, by not deviating too much from a reasonable prior. This framework provides a principled way to analyze and potentially control for phenomena like "overthinking" by viewing it as a form of overfitting, which would correspond to a large $\text{KL}(Q||P)$ term.

Theorem C.12 provides a powerful, high-probability upper bound on the expected reasoning generalization error for policies sampled from the learned posterior Q . While this PAC-Bayesian bound is a valid, generic result, we can derive a more specific bound by using information theory, a perspective that connects the generalization error to the mutual information between the learned policy and the training data. This approach leads to the information-theoretic upper bound in Theorem B.1.

We continue to provide the proof of Theorem B.1 here.

Proof. The core idea is that a policy can only overfit to the training set $S = \{q_1, \dots, q_n\}$ by encoding information about S within its own parameters. The mutual information $I(\pi; S)$ precisely quantifies this amount of encoded information. A key result from learning theory provides the following bound on the expected generalization error:

Lemma C.14. (Information-theoretical generalization upper bound (Xu & Raginsky, 2017).) *With CoT-Space defined above, if the policy π is trained on an i.i.d. drawn training set S with size n , the following upper bound for the reasoning generalization error holds:*

$$|\mathbb{E}[R(\pi) - \hat{R}_n(\pi)]| \leq \sqrt{\frac{C_{max}^2 \cdot I(\pi; S)}{2n}},$$

where C_{max} is the maximum possible value of the reasoning loss $C(\cdot)$, and the expectation is over the random draw of the training set S and the (potentially stochastic) output π of the learning algorithm.

Lemma C.14 transforms the problem of bounding generalization error into the problem of bounding the mutual information $I(\pi; S)$. To make this bound meaningful for our framework, we must connect $I(\pi; S)$ to the structural properties of the generated Chain-of-Thought.

We then turn to bound mutual information by CoT complexity. The policy π expresses the information it has learned from S by generating a CoT, which is a sequence of reasoning steps $\xi = (\xi_1, \xi_2, \dots, \xi_L)$. Each step ξ_i is, in turn, a sequence of tokens. The total information capacity of the policy’s output is therefore determined not just by the number of steps, but by the total number of tokens generated.

Let us define:

- L : The number of reasoning steps in a CoT.
- $|\xi_i|$: The number of tokens in the i -th reasoning step.
- $\sum_{i=1}^L |\xi_i|$: The total number of tokens in the CoT.

The mutual information $I(\pi; S)$ is upper-bounded by the entropy of the policy’s output, which represents its description length or information capacity. The total number of token-level decisions the policy makes determines this capacity. Let $\mathbb{E}[L]$ be the expected number of reasoning steps (reasoning depth) and $\mathbb{E}[|\xi|]$ be the expected number of tokens per step (step verbosity). The expected total number of tokens is $\mathbb{E}[L] \cdot \mathbb{E}[|\xi|]$.

If we assume the policy generates tokens from a dictionary \mathcal{A} , the information required to specify one token is at most $\log |\mathcal{A}|$. Therefore, we can establish the following upper bound on the mutual information.

Lemma C.15. *In LLM reasoning scenarios, if the policy π is trained on a training set S , the mutual information $I(\pi; S)$ is upper bounded as follows:*

$$I(\pi; S) \leq \mathbb{E}_{S, \pi} \left[\sum_{i=1}^L |\xi_i| \right] \cdot \log |\mathcal{A}| = (\mathbb{E}[L] \cdot \mathbb{E}[|\xi|]) \cdot \log |\mathcal{A}|.$$

Lemma C.15 formalizes the intuition that the information a policy learns from data cannot exceed the information content it is capable of expressing in its output.

Together with Lemma C.14, this finishes the proof. □

C.8. Proof of Theorem B.2

Proof. To formalize this, we quantify the notion of problem complexity and establish a condition for policy failure.

Definition C.16. (Required reasoning depth.) For any given query q , we define its *Required Reasoning Depth*, denoted as $L^*(q)$, as the minimum number of CoT steps required to reach any success state $m \in M_q$ from the initial state (q, \emptyset) . This value is an intrinsic property of the query’s complexity.

Definition C.16 can be likened to the minimum number of steps required to solve a reasoning problem. For instance, a simple two-digit addition problem might require only one or two mental steps, making its L^* very low. In contrast, proving a complex theorem, such as the Pythagorean theorem, requires a sequence of many interconnected logical steps, resulting in a high L^* . A policy that attempts to solve the theorem with only a few steps, regardless of how smart it is, will inevitably fail.

Building on the concept of L^* , we now formalize the direct consequence of a policy’s generated reasoning being too shallow. We make a straightforward assumption about the relationship between insufficient reasoning depth and policy failure, which translates a structural property of the CoT into a quantifiable error.

Assumption C.17. (Policy failure on insufficient depth) When a policy π generates a CoT of length L_i for a query q_i , if the length is insufficient to solve the problem, i.e., $L_i < L^*(q_i)$, the policy is guaranteed to fail. The resulting reasoning loss $C(s_{q_i}^\pi)$ is therefore bounded below by a significant positive constant, which we denote as $C_{fail} > 0$. In the worst case, this loss can be as high as C_{max} .

Assumption C.17 claims that a policy’s failure due to insufficient depth can be observed in practice. Consider a complex physics problem requiring multiple steps: identifying the forces, setting up equations, and solving for variables. A policy that only completes the first step and then stops will not be able to reach the correct final answer. In this case, the loss function would assign a high penalty (our C_{fail}) because the generated CoT, while possibly correct for the initial step, is fundamentally incomplete for solving the problem. The policy, therefore, cannot even fit the training data for problems that require deeper reasoning.

Building upon Definition C.16 and Assumption C.17, we can then derive a lower bound of the empirical reasoning loss $\hat{R}_n(\pi)$.

We begin with its definition:

$$\hat{R}_n(\pi) = \frac{1}{n} \sum_{i=1}^n C(s_{q_i}^\pi). \quad (60)$$

We can partition the sum over the training set into two disjoint subsets based on whether the generated CoT length was sufficient:

- The set of failed queries: $S_{fail} = \{q_i \in S \mid L_i < L^*(q_i)\}$.
- The set of potentially successful queries: $S_{succ} = \{q_i \in S \mid L_i \geq L^*(q_i)\}$.

Let $n_{fail} = |S_{fail}|$. We can now rewrite the empirical loss as:

$$\hat{R}_n(\pi) = \frac{1}{n} \left(\sum_{q_i \in S_{fail}} C(s_{q_i}^\pi) + \sum_{q_i \in S_{succ}} C(s_{q_i}^\pi) \right). \quad (61)$$

Applying our failure assumption, we know that for every $q_i \in S_{fail}$, $C(s_{q_i}^\pi) \geq C_{fail}$. For queries in S_{succ} , the loss is at least 0. This allows us to establish a lower bound:

$$\hat{R}_n(\pi) \geq \frac{1}{n} \left(\sum_{q_i \in S_{fail}} C_{fail} + \sum_{q_i \in S_{succ}} 0 \right) = \frac{n_{fail} \cdot C_{fail}}{n}. \quad (62)$$

We can define the empirical failure rate of the policy π on the training set as $P_\pi(L < L^*) = n_{fail}/n$. This leads to our final lower bound for the empirical loss:

$$\hat{R}_n(\pi) \geq P_\pi(L < L^*) \cdot C_{fail}. \quad (63)$$

This finishes the proof. □

D. Experimental Settings

Dataset The experiments are conducted on the MATH (Hendrycks et al., 2021) and GSM8K (Cobbe et al., 2021) benchmarks. The MATH training set is manually subdivided into five difficulty levels (Level 1–5) according to the original “level” field, where Level 5 is substantially more challenging than Level 1.

Base Model A diverse collection of pre-trained LLMs with varying architectures, parameter counts, and versions serves as the reference model for the reinforcement-learning algorithms. Specifically, the models include

- **Qwen2.5 series** (Qwen, 2025a): Qwen2.5-7B, Qwen2.5-3B, Qwen2.5-1.5B, and Qwen2.5-0.6B.
- **Qwen3 series** (Qwen, 2025b): Qwen3-8B-Base, Qwen3-4B-Base, Qwen3-1.7B-Base, and Qwen3-0.6B-Base.
- **Llama3 series** (Meta, 2024): Llama-3.1-8B-Instruct, Llama-3.2-3B-Instruct, and Llama-3.2-1B-Instruct.

The maximum response length is set to 2,048 tokens for the Qwen2.5 and Llama3 models and to 8,196 tokens for the reasoning-intensive Qwen3 models.

Algorithm and Hyperparameters The evaluation covers the current mainstream reinforcement-learning algorithms for mathematical reasoning: GRPO (Shao et al., 2024), PPO (Schulman et al., 2017), DAPO (Yu et al., 2025), Reinforce++ (Hu et al., 2025), and RLOO (Ahmadian et al., 2024). The reward function is rule-based (DeepSeek-AI, 2025). For PPO, the critic model is initialized from Qwen2.5-0.6B. The learning rate for critic training is 1×10^{-5} , the k3 KL-regularization coefficient is 0.001, and the GAE parameters λ and γ are both set to 1. For DAPO, no KL regularization is applied; the high and low clip ratios are 0.28 and 0.20, respectively, and L_{cache} is 1,024. Across all algorithms, each training sample is sampled eight times ($K = 8$). The actor is optimized with AdamW (Loshchilov & Hutter, 2017) at a learning rate of $1e-6$, the training batch size is 128, and training proceeds in a purely on-policy manner for up to 50 steps. All experiments are run on 8×96 GB NVIDIA H20 GPUs.

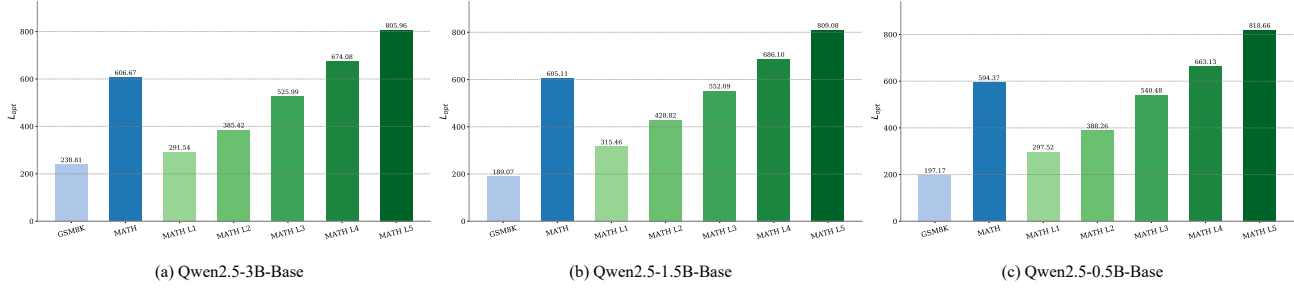


Figure 6. **Supplementary validation of the relationship between task difficulty and optimal CoT length (L_{opt}) on additional models.** The plots illustrate that the converged mean response length (L_{opt}) consistently increases with task difficulty across three different models: (a) Qwen2.5-3B-Base, (b) Qwen2.5-1.5B-Base, and (c) Qwen2.5-0.5B-Base. These results reinforce the findings presented in Figure 5(a) and demonstrate the robustness of Remark 1 across models of varying capacities.

E. More Experiments

To further strengthen the empirical validation of Remark 1, we conducted supplementary experiments to verify the relationship between task difficulty and the optimal CoT length (L_{opt}) across models of varying capacities. The experimental protocol is identical to that described in Section 4, but here we replicate the analysis on three additional models from the Qwen2.5 series: Qwen2.5-3B-Base, Qwen2.5-1.5B-Base, and Qwen2.5-0.5B-Base.

The results, presented in Figure 6, consistently corroborate the findings from our main experiment (Figure 5(a)). Across all three smaller models, we observe the same clear, monotonic trend: the converged optimal CoT length (L_{opt}) increases systematically as the difficulty of the task escalates from GSM8K to the higher levels of the MATH dataset. This demonstrates that the principle outlined in Remark 1, that more complex problems necessitate a longer reasoning process to avoid underfitting is not specific to a single high-capacity model but holds true as a general principle across models of different scales.

F. Broader Explanatory Power of CoT-Space

This section further explores the extensibility of the CoT-Space framework, demonstrating its capacity to provide a unified theoretical account for several other critical and complex phenomena observed in LLMs, beyond the “overthinking” problem analyzed in the main body of this paper.

F.1. Hallucination as Trapped Optimization in Phantom Minima

The phenomenon of hallucination (Ji et al., 2023), where a model generates fluent but factually incorrect statements, can be elegantly re-contextualized within our framework. In CoT-Space, reasoning is modeled as an optimization process on a continuous semantic manifold, aimed at minimizing a reasoning loss function $C(s)$. An ideal reasoning trajectory converges to a global minimum M_g , which corresponds to the correct solution. Hallucination can thus be explained as the optimization trajectory becoming trapped in a “phantom minimum” or a deep local minimum within the loss landscape. These states, while possessing a low reasoning loss due to their local coherence and syntactical correctness, do not correspond to the ground truth. Once a model’s reasoning state s_t enters the basin of attraction for such a trap, subsequent gradient-like updates will cause it to converge there, rather than to the true global minimum, yielding a chain-of-thought that is internally consistent but externally false.

F.2. Prompt Sensitivity as a Consequence of Landscape Instability

Furthermore, the acute sensitivity of LLMs to minor, semantically irrelevant perturbations in the input prompt (Zhuo et al., 2024; Razavi et al., 2025) can be understood as an initial state perturbation problem on an unstable loss landscape. The input query q defines the initial state of the reasoning process, $s_0 = (q, \emptyset)$, which serves as the starting point for the optimization trajectory. The high-dimensional, non-convex loss landscape is likely replete with unstable topological features such as sharp ridges, crevasses, or watersheds. If an initial state s_0 is located near such an unstable region, a slight perturbation of the prompt (from q to q') can shift the initial state to s'_0 . Although the distance between s_0 and s'_0 in the semantic space may be negligible, they might lie on opposite sides of a watershed. Consequently, their subsequent optimization trajectories will

follow entirely different descent paths, converging to distinct minima and producing dramatically different outputs. This provides a formal, geometric interpretation for the model’s apparent brittleness.

F.3. Emergent Abilities as a Topological Phase Transition

The framework also offers a compelling explanation for the “emergent abilities” of LLMs, where complex reasoning capabilities appear to manifest suddenly once model scale surpasses a certain threshold, a phenomenon often described as a “reasoning cliff” for smaller models (Wei et al., 2022a). This can be interpreted as a change in the topological properties of the reasoning space itself, which is directly influenced by model capacity. Smaller models, with their limited representational power, exhibit a lower reasoning state density $\rho(K)$, as defined in Definition 2.8. As established in Theorem 2.12, a low density implies a larger expected distance between adjacent states, rendering the corresponding semantic manifold \tilde{S} sparse, perforated, or even disconnected. For a complex problem, the path from the initial state s_0 to the solution M_q may contain unbridgeable gaps, precluding any successful optimization trajectory and thus creating the reasoning cliff. As model scale increases, the representational capacity grows, leading to an exponential increase in the state density $\rho(K)$. This makes the manifold progressively more dense and smooth, effectively “filling in the holes” and establishing continuous pathways for reasoning. The emergence of an ability corresponds to a topological phase transition, where the manifold’s connectivity reaches a critical point that permits a viable optimization process.

F.4. The Efficacy of External Slow-Thinking

Finally, CoT-Space provides a principled basis for the superior performance of external slow-thinking strategies like ToT (Yao et al., 2023) or MCTS (Wan et al., 2024) compared to standard CoT. The difference in their efficacy can be framed as the difference between two optimization algorithms operating on the same loss landscape. Standard CoT generation is analogous to a greedy, single-path gradient descent. At each step, it commits to a single, locally optimal thought, following a solitary trajectory that is highly susceptible to being trapped in the first local minimum it encounters. In contrast, external slow-thinking strategies maintain multiple parallel candidate reasoning paths. This is equivalent to performing a beam search within the semantic state space. By exploring multiple descent directions from a given state s_t , external slow-thinking strategies conduct a more comprehensive exploration of the complex, non-convex loss landscape. This strategy significantly enhances the probability of circumventing local traps and identifying a path to the global optimum, thereby explaining its enhanced effectiveness on complex reasoning tasks.

G. Prescriptive Implications

Beyond explaining current phenomena, CoT-Space provides a theoretical justification for Latent Space Reasoning. Since we prove that the reasoning space converges to a continuous manifold \tilde{S} , it is theoretically sound to map discrete CoT steps into this continuous latent space (e.g., via variational auto-encoders). Optimization (reasoning) could then be performed via gradient-based planning in this smooth latent space, avoiding the discrete, non-differentiable nature of token generation, before decoding the final result. Furthermore, our framework suggests that current sparse reward models are inefficient proxies for the smooth reasoning loss $C(s, q)$. Future work should focus on training Continuous Verifiers that predict a scalar “semantic distance” to the solution, providing the dense, smooth gradients required for more stable RL optimization.